

# The cyclic phase transformations in Fe-X-C alloys

**Hao Chen, Sybrand van der Zwaag**

*Novel Aerospace Materials group*

*Faculty of Aerospace Engineering, Delft University of Technology*

In collaboration with **Goune Mohamed**, Arcelor-Mittal, France and **Benoit Appolaire**, Onera, France

# The kinetics of austenite to ferrite transformation :

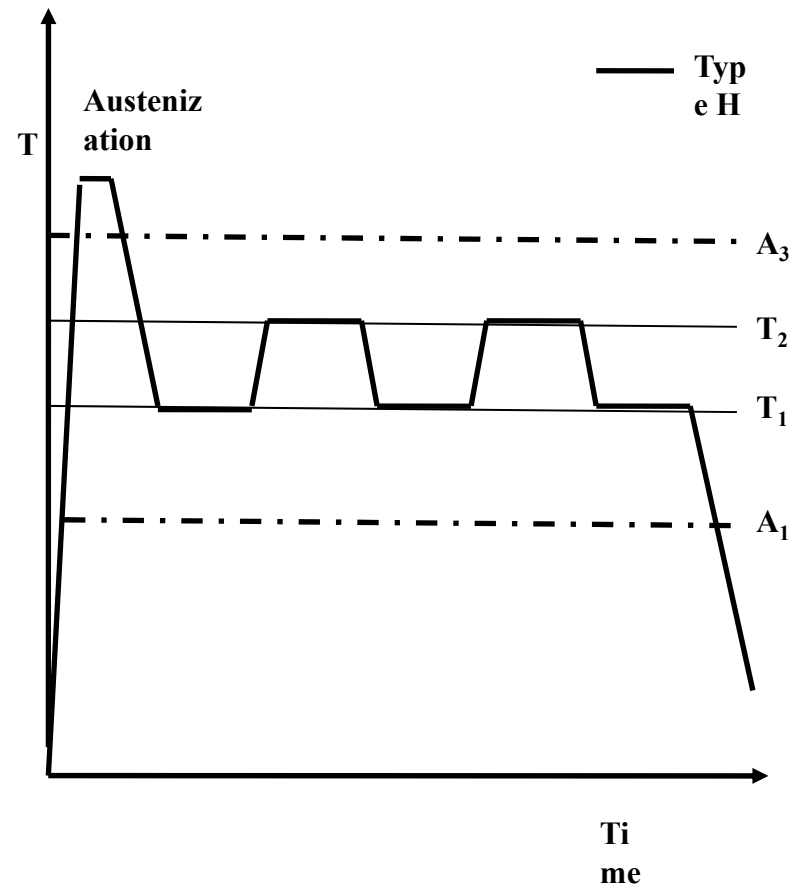
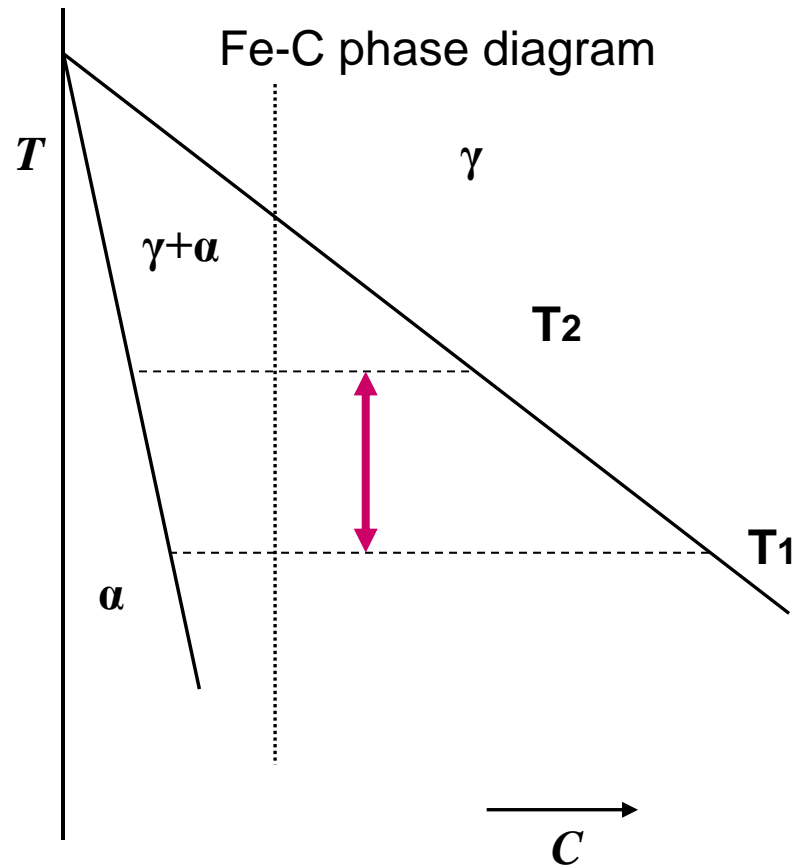
1. includes nucleation and growth, which may overlap.
2. Has a nucleation mechanism which is difficult to be determined.
3. Has a growth mechanism which is controlled by diffusion, interface migration or a combination of both

# The challenge and aim in this work

Design an experiment which enable determination of growth kinetics for the austenite to ferrite phase transformation and vice versa more accurately:

1. Obtaining more accurate value of interface mobility
2. Validating the different models

# The cyclic partial transformation concept



# The cyclic partial phase transformation concept

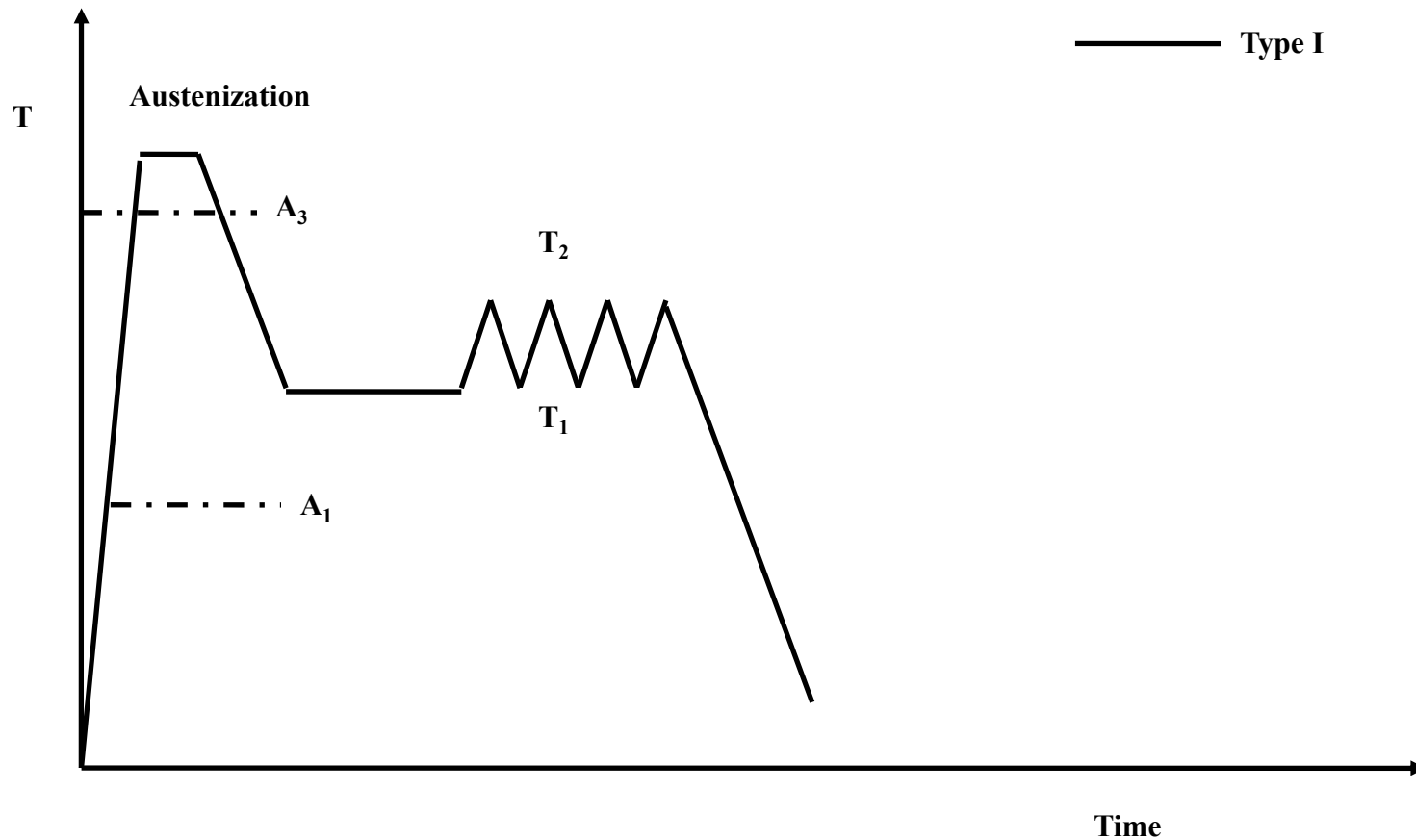
The advantages :

1. Ferrite nucleation effects can be suppressed
2. The interface mobility for both the austenite to ferrite and ferrite to austenite transformation can be determined.
3. The pure ferrite to austenite transformation can be studied as the pearlite dissolution process is avoided.

# Results to be presented

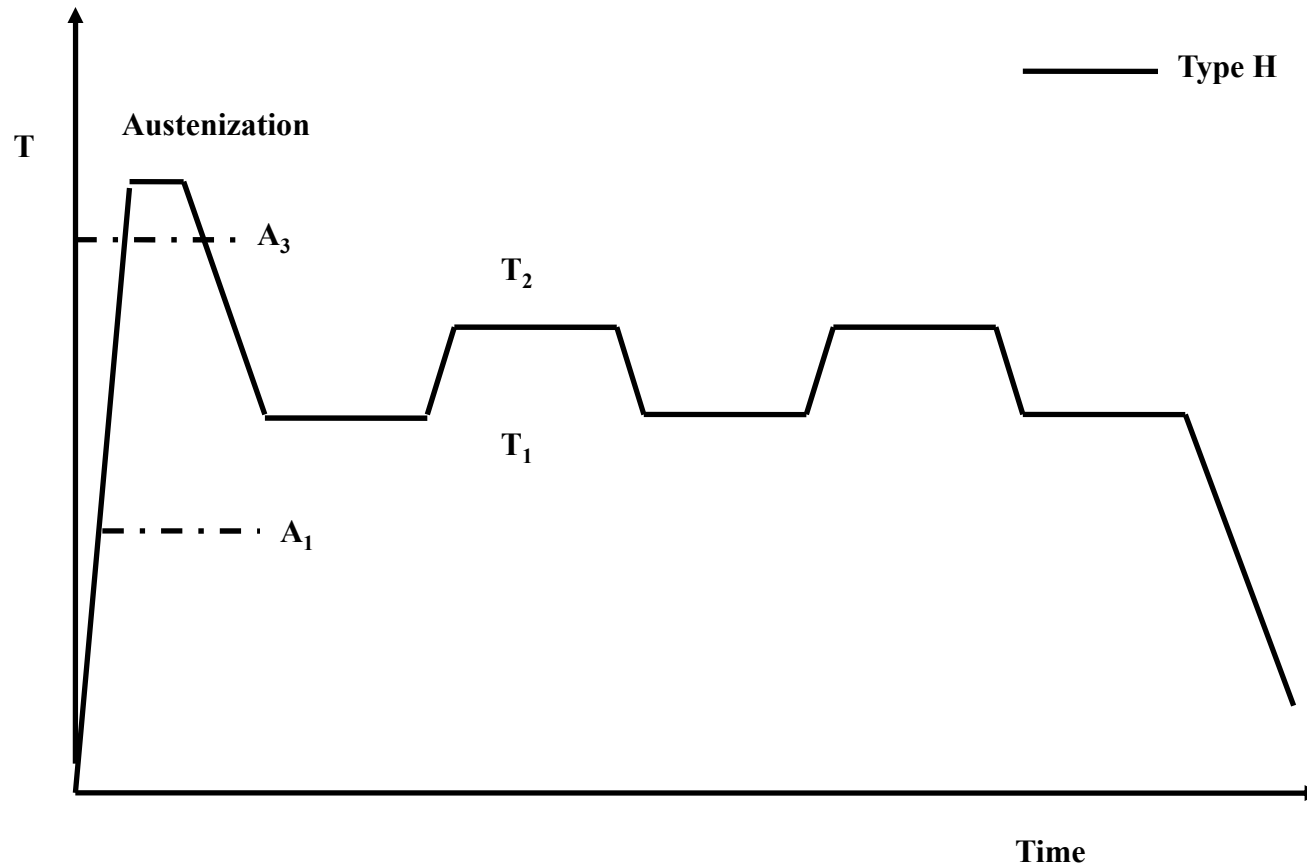
- 1- cyclic transformation curves at 10 K/min for a Fe-0.17Mn-0.02C alloy
- 2- comparison with PE and LE calculations
- 3- effects of heating and cooling rate on the stagnant and inverse transformation
- 4- calculated behavior of ternary Fe-X-0.02 C alloys for X = Mn, Ni, Cu, Si,Co
- 5- creating experimental indirect evidence for the Mn spike at the moving interface

# Immediate (type I) Cyclic Phase transformations for Fe-Mn-C



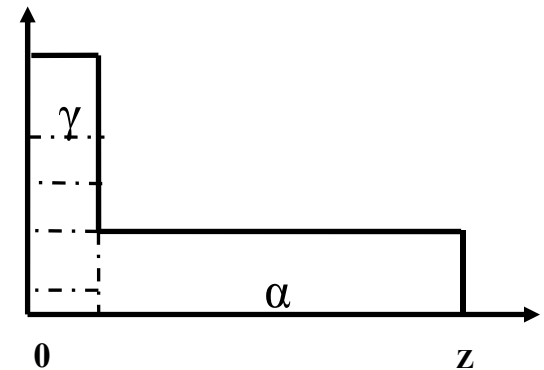
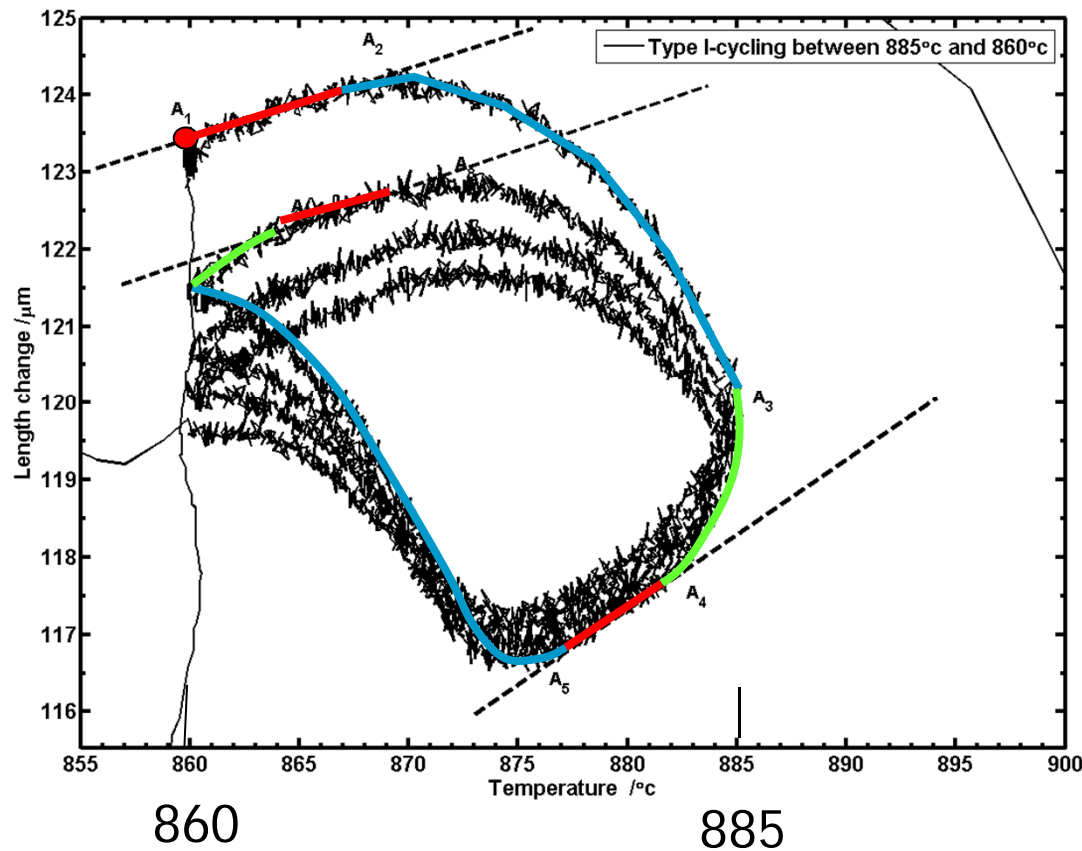
# Holding (type H)

## Cyclic phase transformations for Fe-Mn-C



# Experimental results for a **type I** experiment

Fe-0.17Mn-0.023C (wt. %) alloy

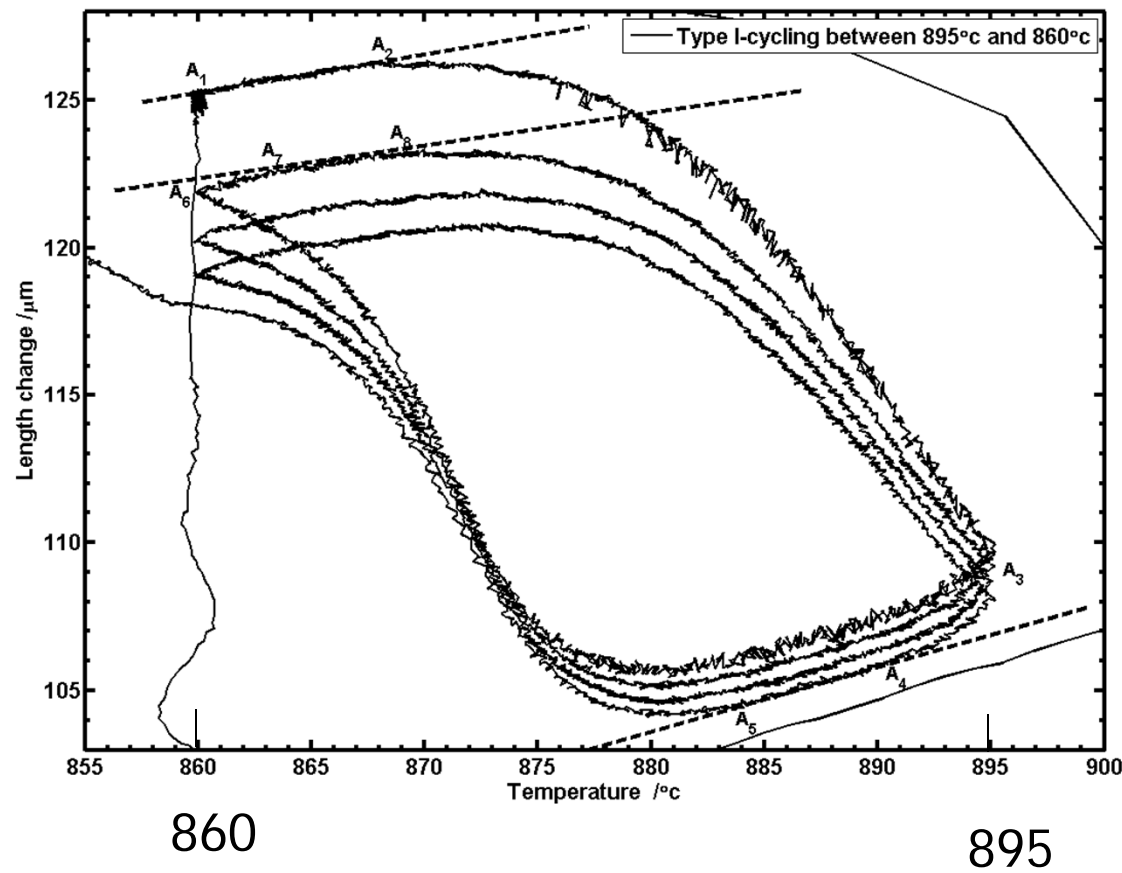


A<sub>1</sub>-A<sub>2</sub> and A<sub>4</sub>-A<sub>5</sub>

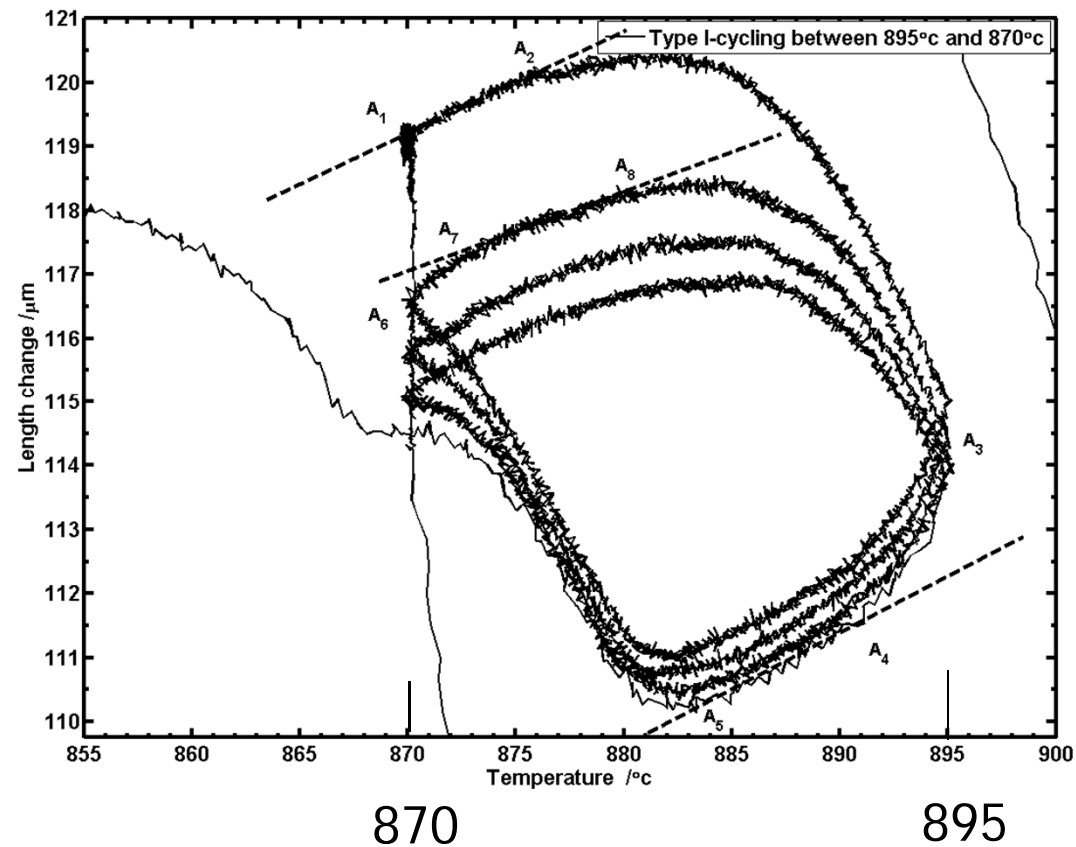
**stagnant stage**

A<sub>3</sub>-A<sub>4</sub> **Inverse phase transformation stage**

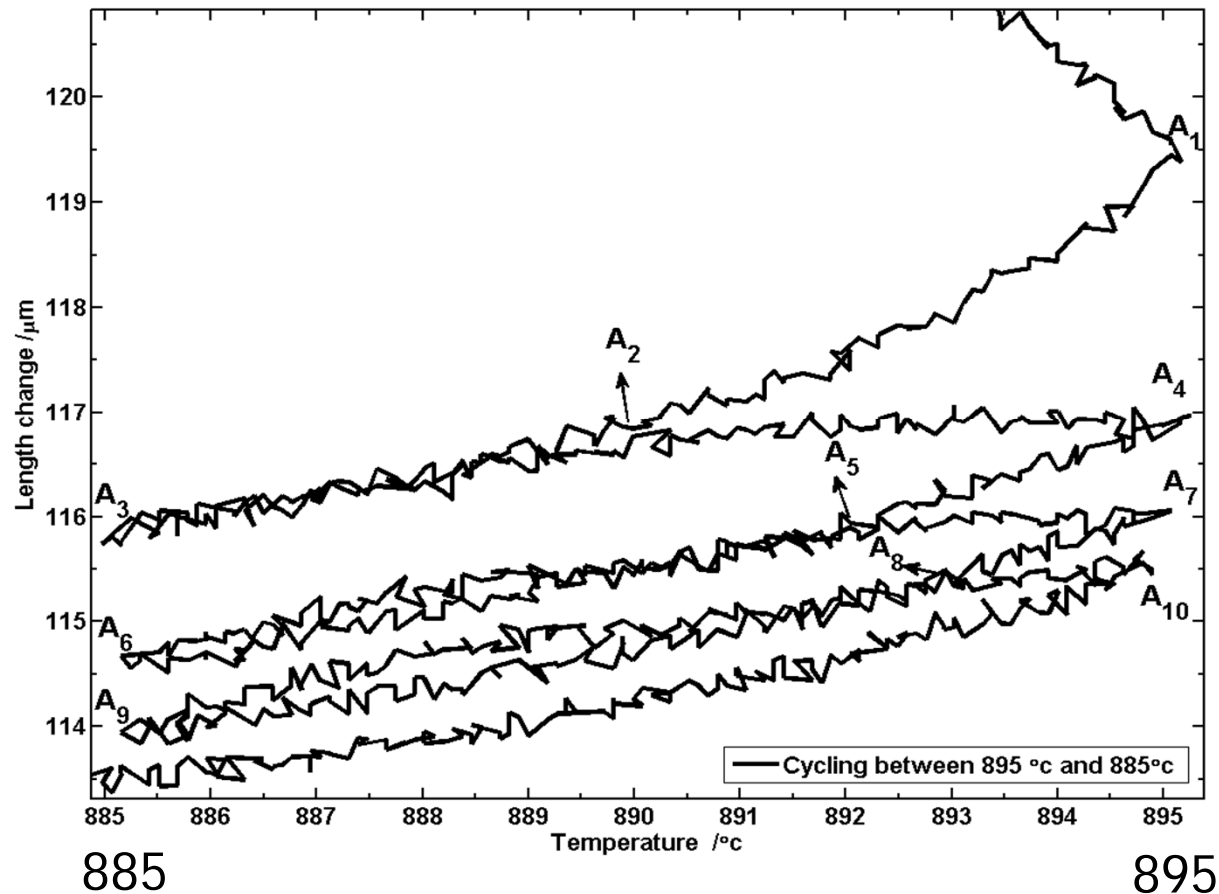
# Results for a larger temperature range



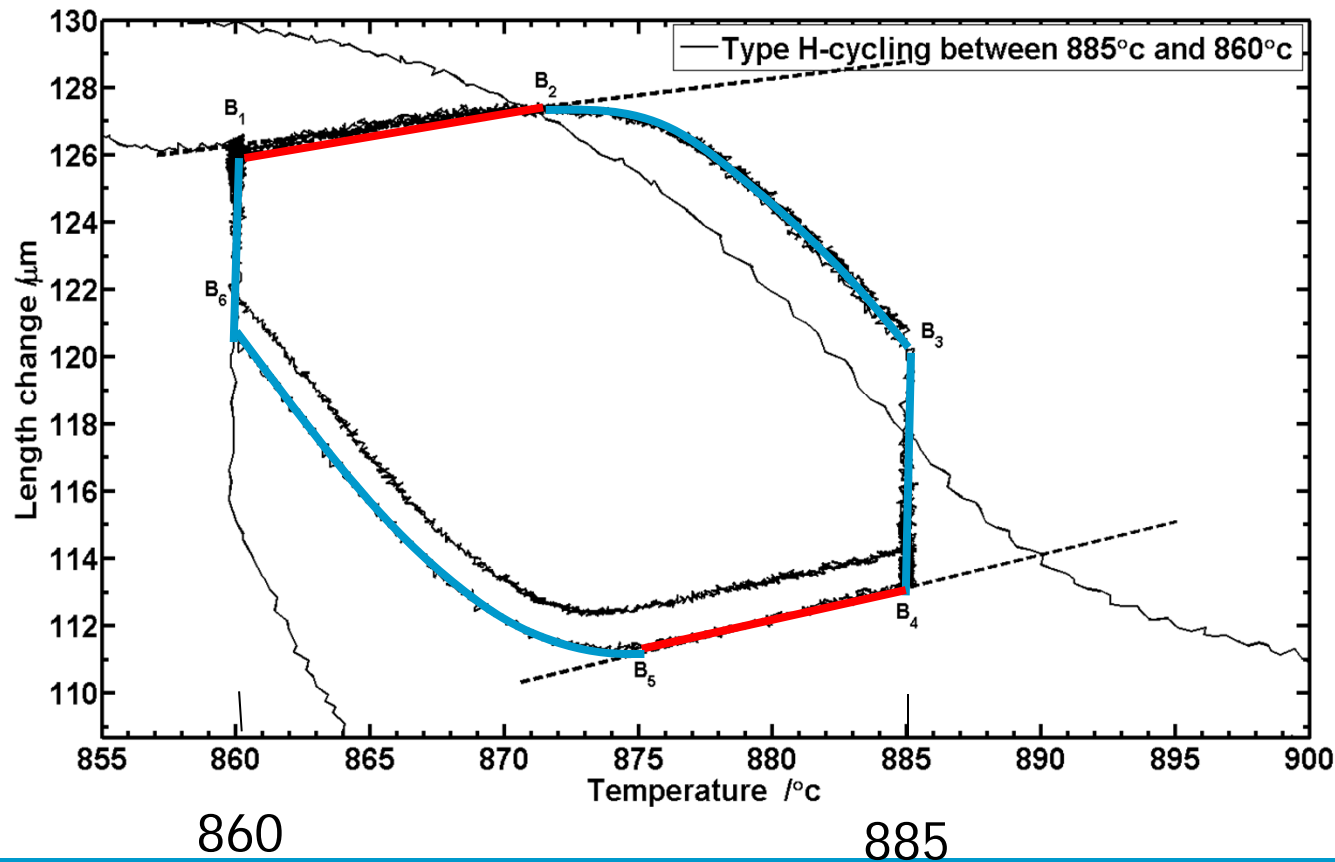
# Results for a smaller temperature range



# Cycling in the stagnant stage



# Experimental results for a **type H** experiment



# Interim summary

Cyclic partial phase transformation experiments show

- **Stagnant** stages during the initial part of the cycle
- **Normal** transformation behaviour during the next part
- **Inverse** transformation stages for type I experiments
- Absence of inverse transformation stages for type H experiments

# Modelling 1

## Local equilibrium model for Fe-C-M (LE-NP and LE-P)

In the LE model, the carbon and the substitutional element M partitionings according to local equilibrium assumptions, which means the chemical potential of carbon and M across the interface should be constant:

$$\mu_i^\gamma = \mu_i^\alpha \quad i=M \text{ or } C$$

Diffusion equations: 
$$\frac{\partial X_i^\phi(r,t)}{\partial t} = \frac{1}{r^{k-1}} \frac{\partial}{\partial r} \left( r^{k-1} D_i^\phi(X_i^\phi(r,t)) \frac{\partial X_i^\phi(r,t)}{\partial r} \right)$$

Boundary conditions: 
$$\left. \frac{\partial X_i^\phi(r,t)}{\partial r} \right|_{r=0}^{r=L} = 0 \quad \Phi = \gamma \text{ or } \alpha \text{ and } i=M \text{ or } C$$

Mass balance at the interface: 
$$J_i^\gamma - J_i^\alpha = v(X_i^\gamma - X_i^\alpha) \quad i=M \text{ or } C$$

# Modelling the cyclic transformations

## Paraequilibrium model for Fe-C-M

In the paraequilibrium model, the substitutional element M does not redistribute and the chemical potential of C is a constant across the interface. The chemical potential equations can be described as:

$$\mu_C^\gamma = \mu_C^\alpha$$

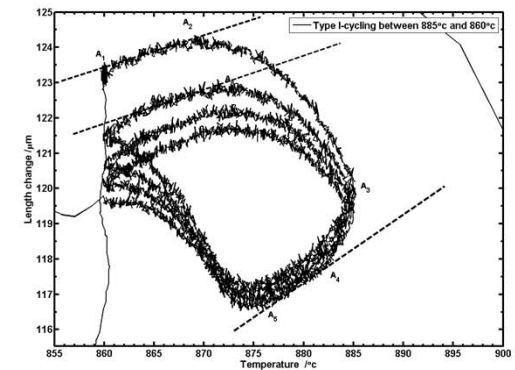
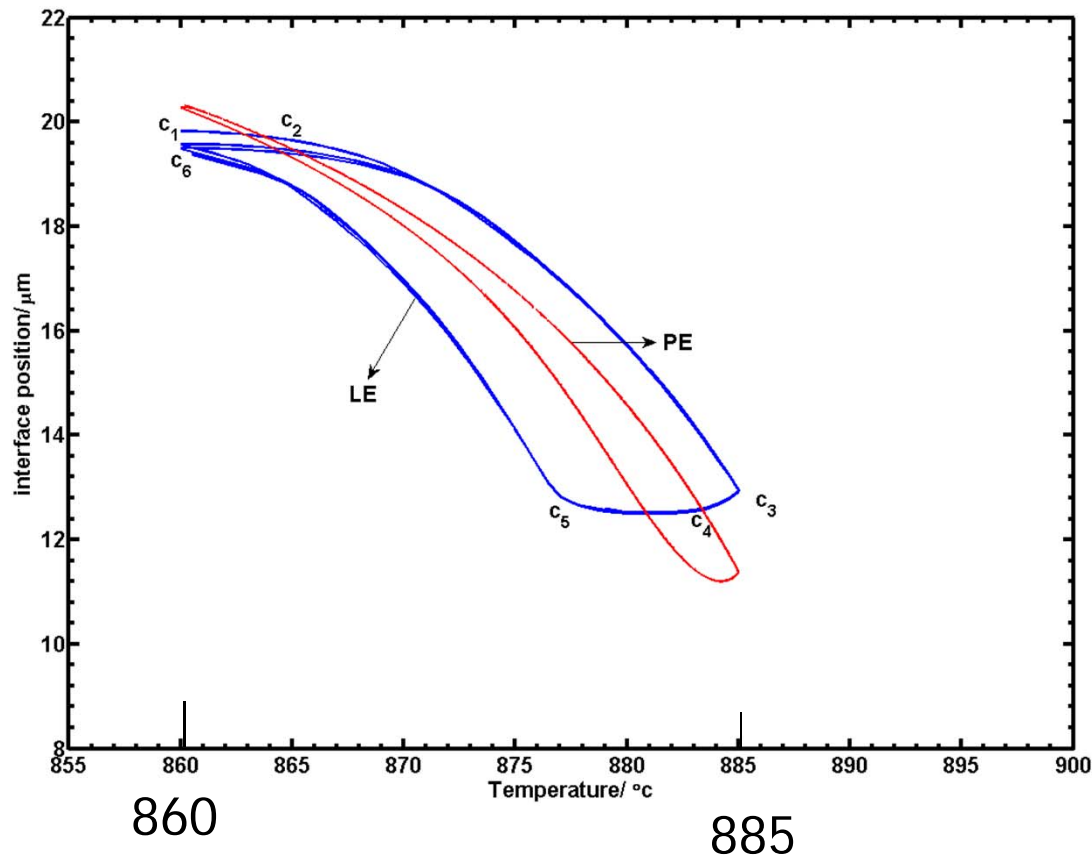
$$(\mu_M^\gamma - \mu_M^\alpha) = -\frac{X_{Fe}}{X_M}(\mu_{Fe}^\gamma - \mu_{Fe}^\alpha)$$

Diffusion equations: 
$$\frac{\partial X_i^\phi(r,t)}{\partial t} = \frac{1}{r^{k-1}} \frac{\partial}{\partial r} \left( r^{k-1} D_i^\phi(X_i^\phi(r,t)) \frac{\partial X_i^\phi(r,t)}{\partial r} \right)$$

Boundary conditions: 
$$\left. \frac{\partial X_i^\phi(r,t)}{\partial r} \right|_{r=0}^{r=L} = 0 \quad \Phi = \gamma \text{ or } \alpha \text{ and } i = C$$

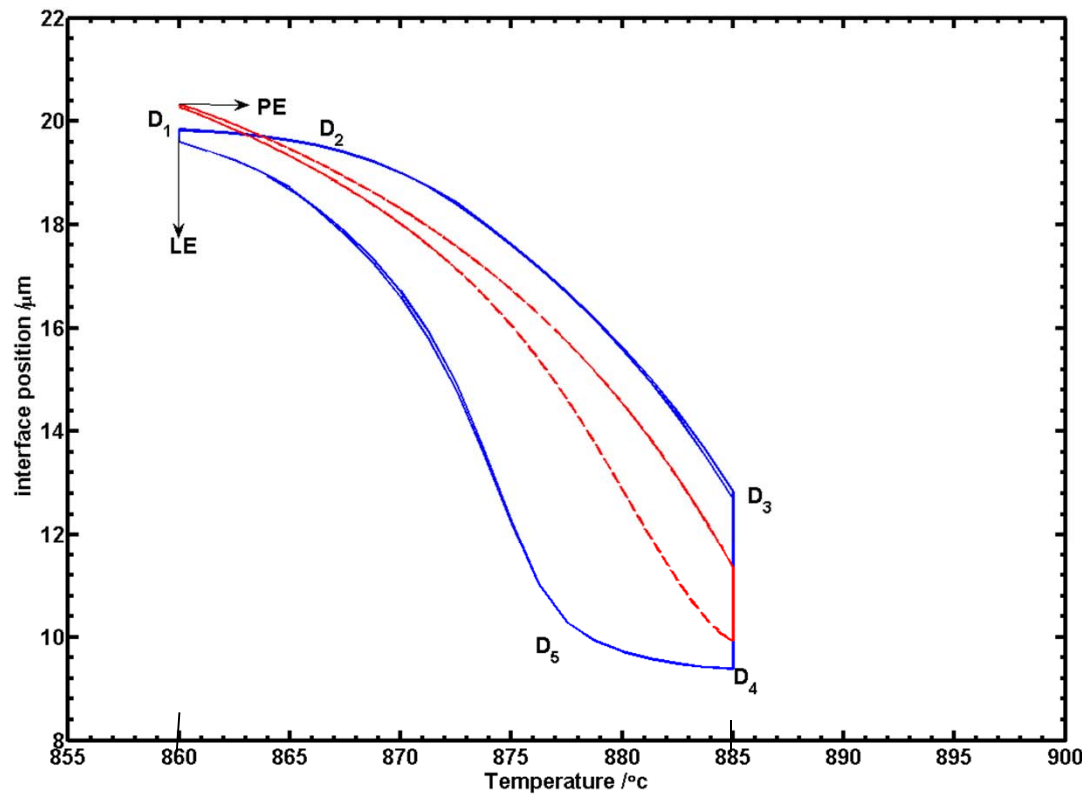
Mass balance at the interface: 
$$J_i^\gamma - J_i^\alpha = v(X_i^\gamma - X_i^\alpha) \quad i = C$$

# Modelling results for type I experiment



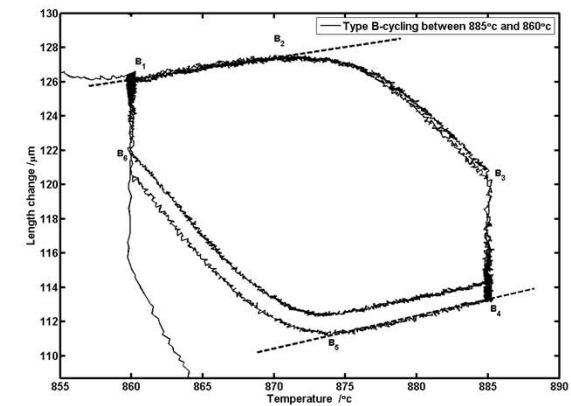
Experimental  
results

# Modelling results for type H experiment



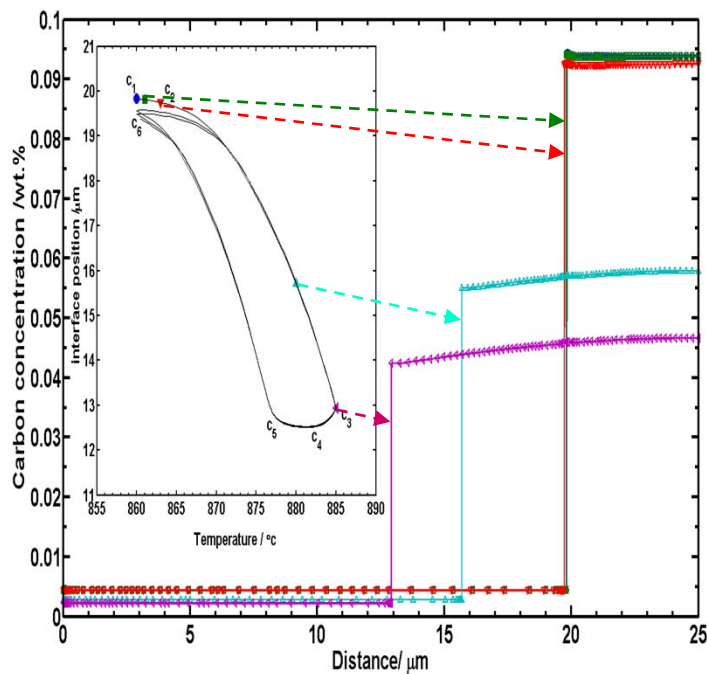
860

885

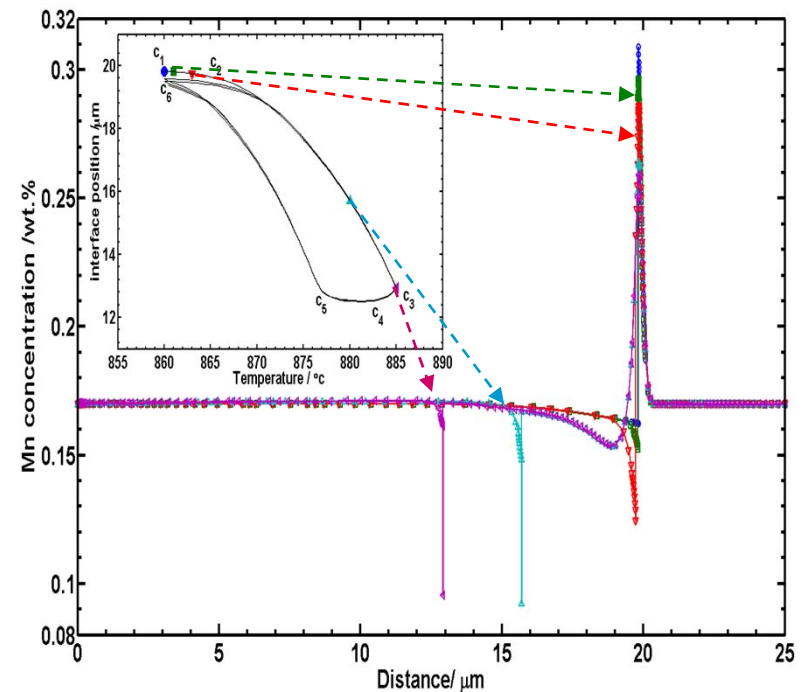


Experimental  
results

# Concentration profiles during 1<sup>st</sup> heating cycle

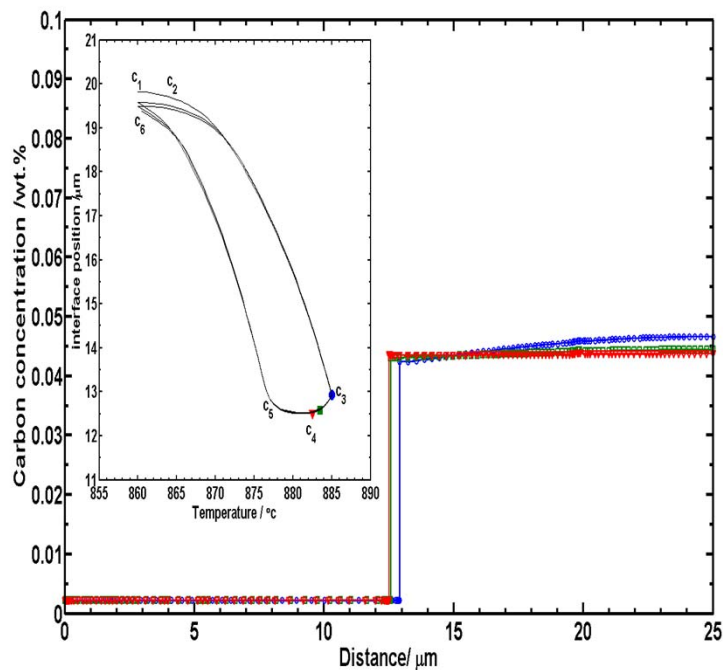


Carbon profiles

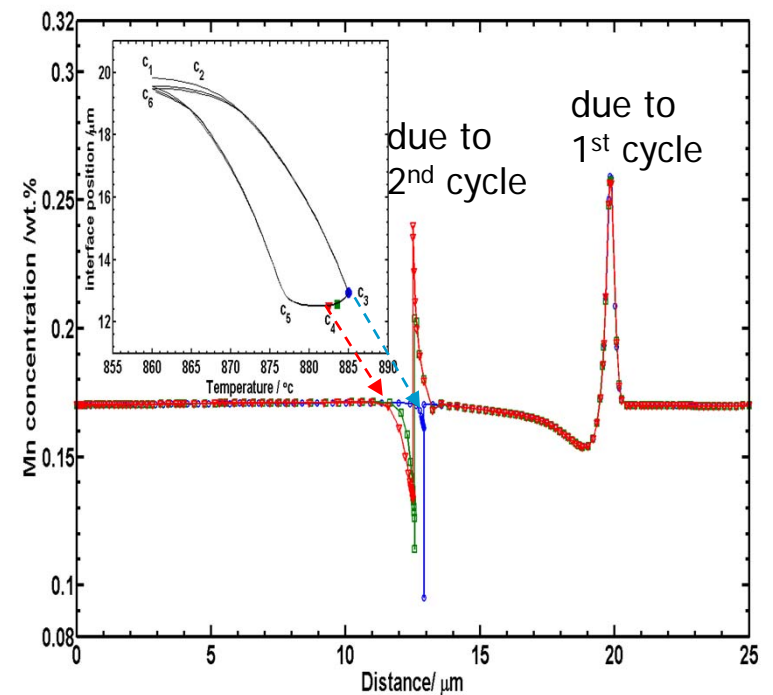


Mn profiles

# Concentration profiles for the 1<sup>st</sup> cooling stage

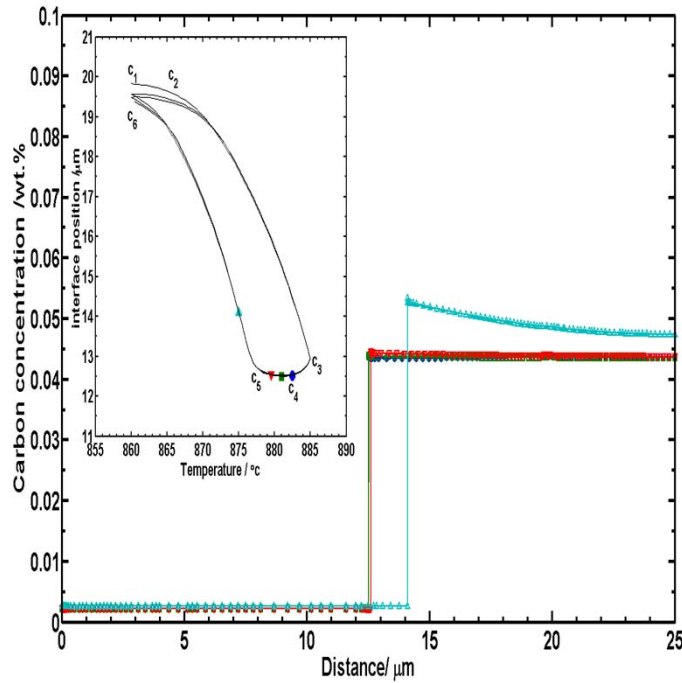


Carbon profile

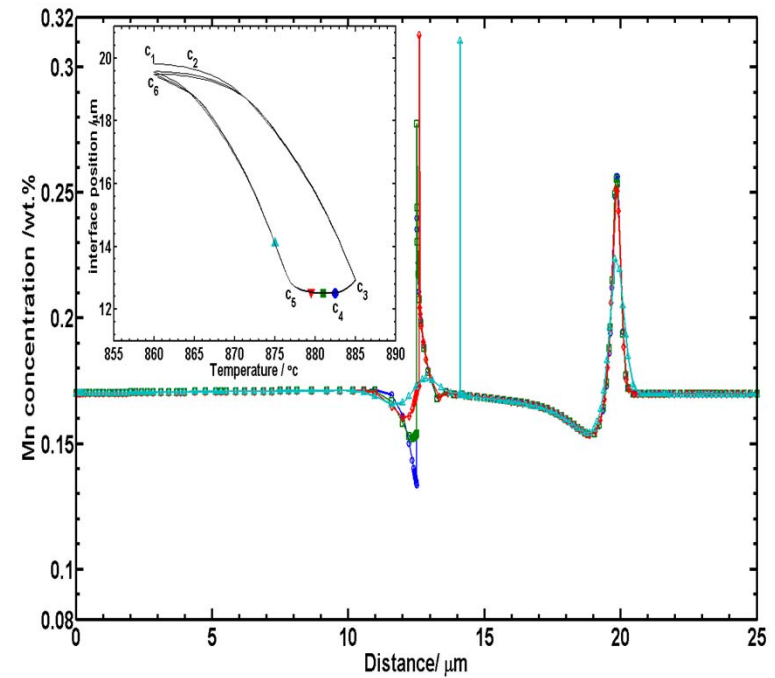


Mn profile

# The stagnant stage in more detail



Carbon profile



Mn profile

# Interim summary

1. The LE model can predict the new features qualitatively, while the PE model does not work at all.
2. The stagnant stage is caused by Mn partitioning at the interface. maybe interface mobility also play a role.
3. The inverse transformation is due to the non-equilibrium conditions at the transition temperature.

# The effect of cooling rate and heating rate on the stagnant stage and inverse transformation stage

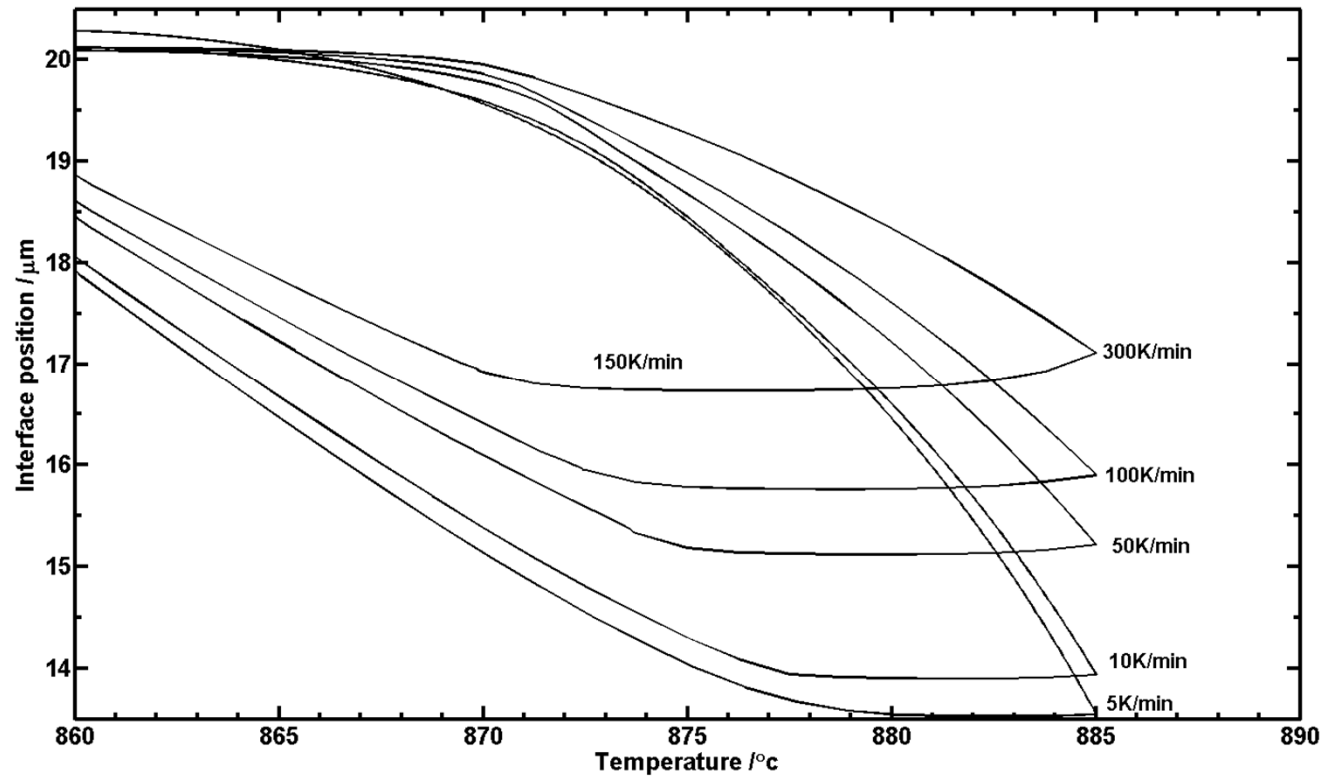
# Simulation

115 different combinations of cooling and heating rate have been simulated by local equilibrium model.

The range of cooling and heating rate is from 5K/min to 1500K/min

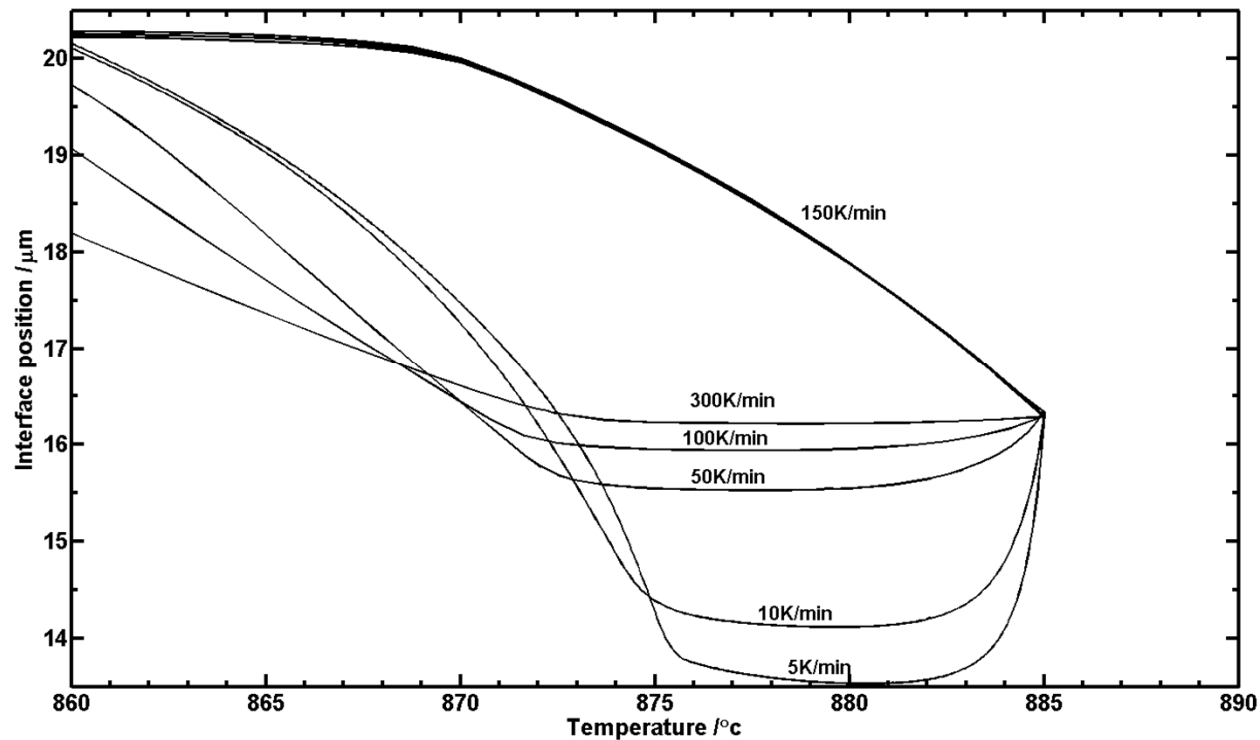
The studied alloy is Fe-0.2Mn-0.02C

# Varying heating rate



Equilibrium interface position at 885C is 11 $\mu\text{m}$

# Varying cooling rate



Equilibrium interface position at 885C is 11 $\mu\text{m}$

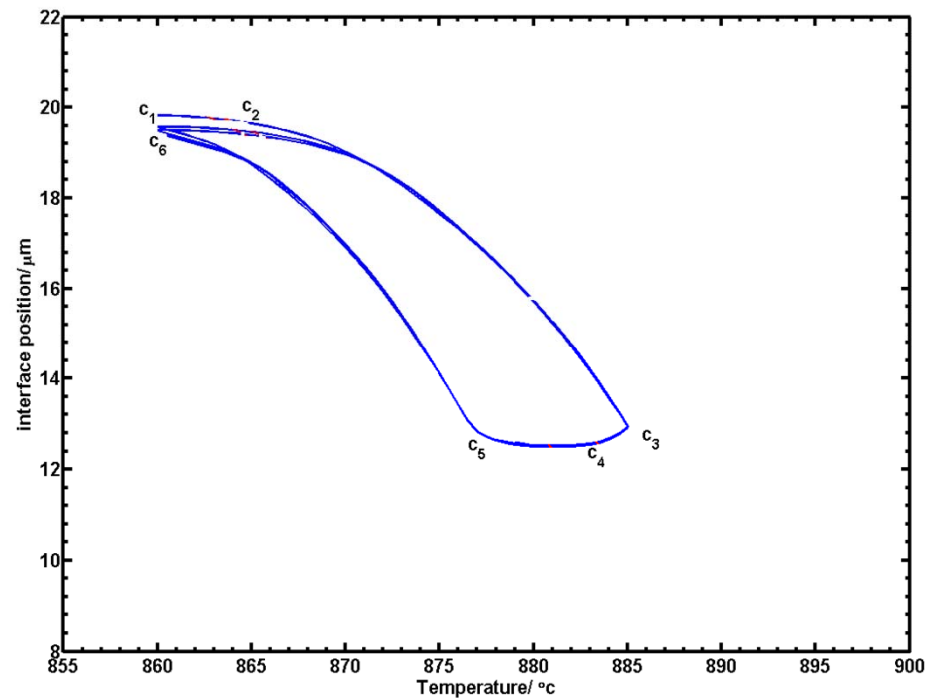
# Definitions

Magnitude of Inverse transformation stage:

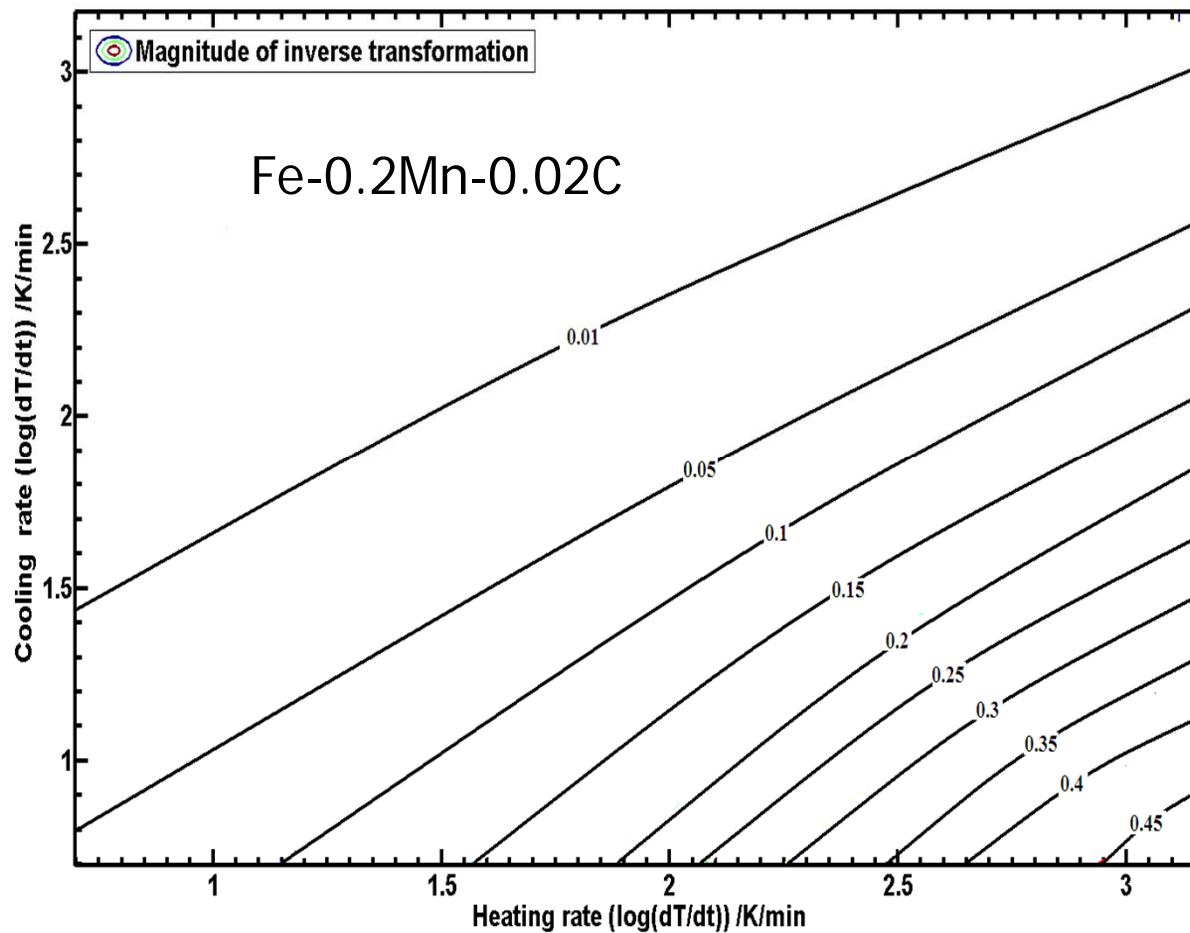
$$= \frac{\Delta f_I^\gamma}{f_{eq}^\gamma(T_2) - f_{eq}^\gamma(T_1)}$$

Length of stagnant stage:

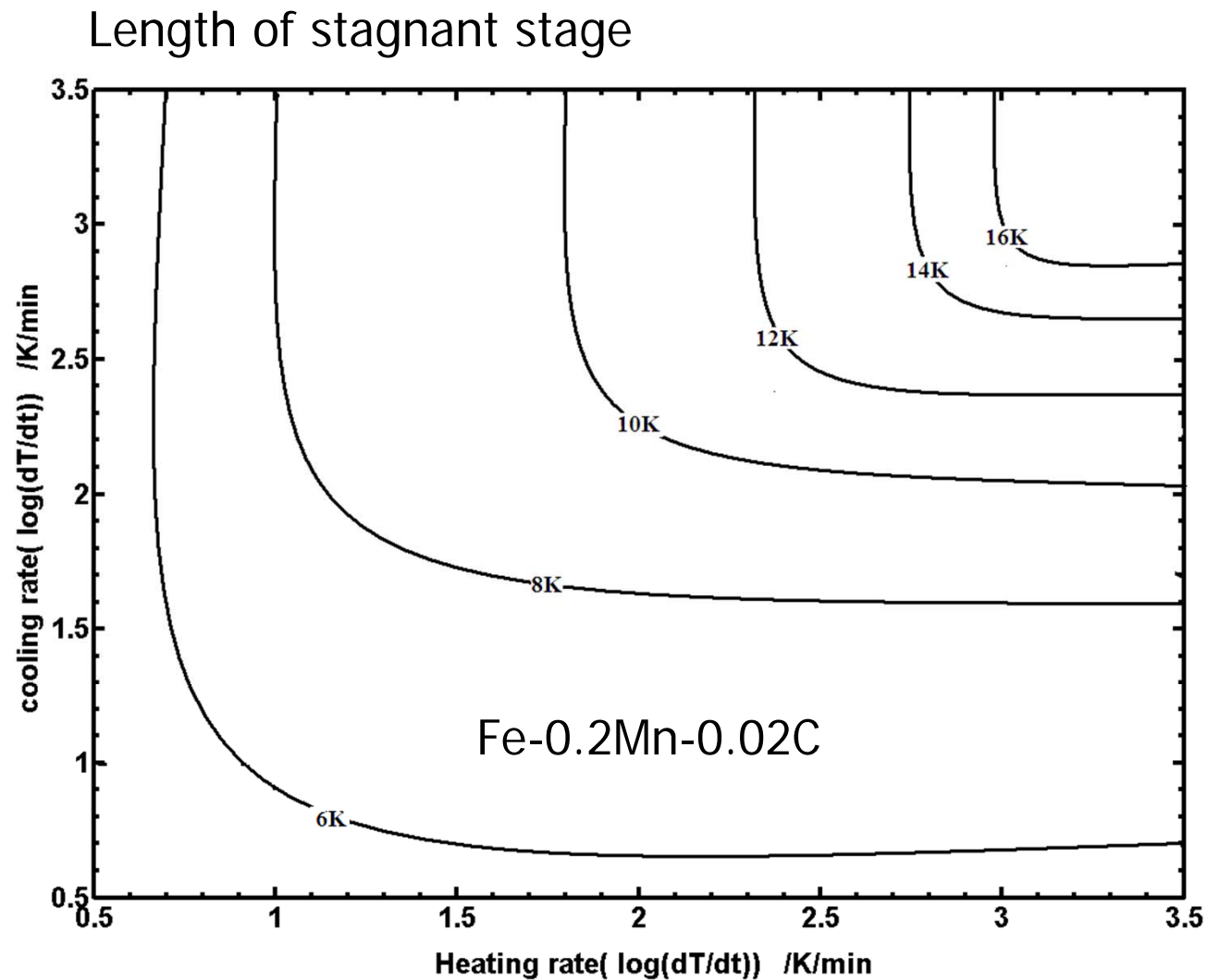
$$\Delta T = T_{C_4} - T_{C_5}$$



# The inverse transformation stage



# The stagnant stage



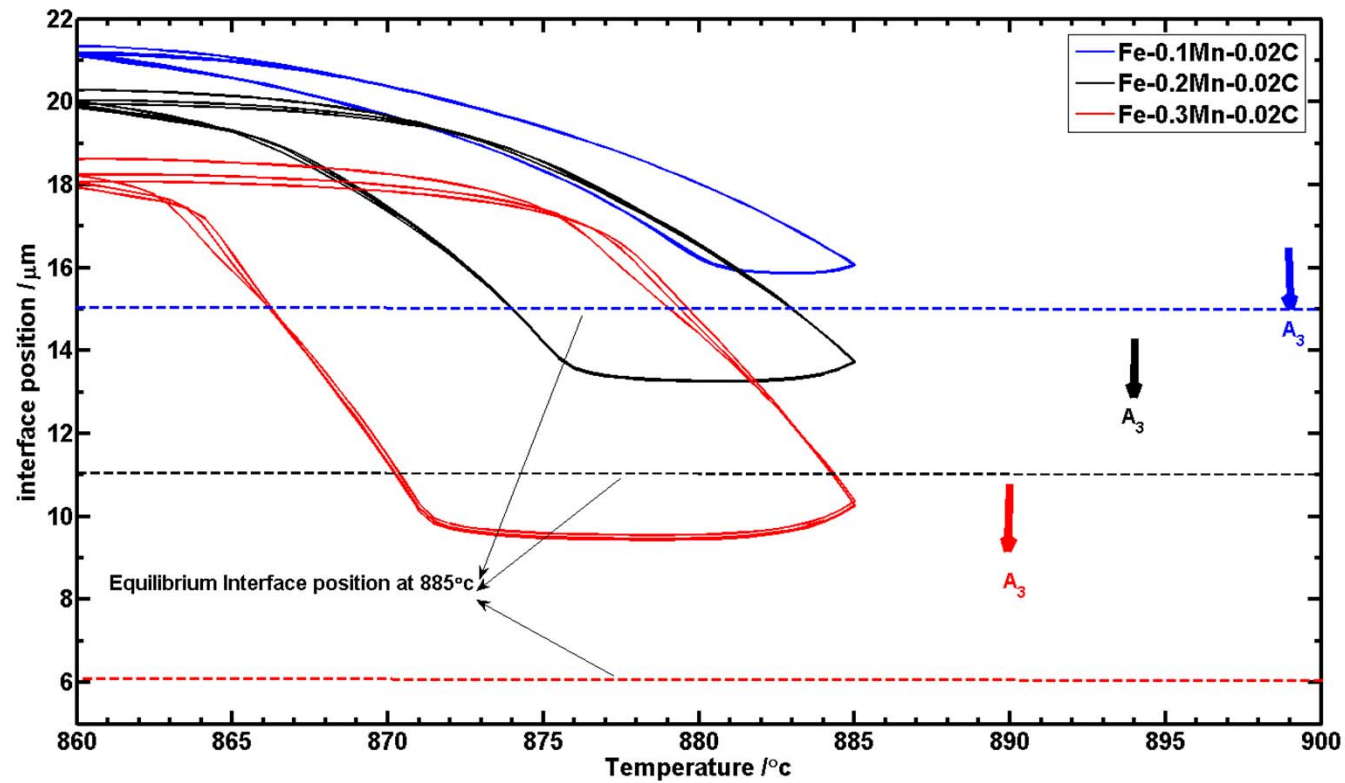
# Interim summary

1. The length of stagnant stage increases with increasing heating rate or increasing cooling rate. The magnitude of inverse transformation increases with increase heating rate and decreasing cooling rate.
2. The length of the stagnant stage is fundamentally determined by the interface conditions after the inverse transformation.
3. The Magnitude of inverse transformation is determined by the interface conditions at  $T_2$  and cooling rate.

# The calculated effect of substitutional element in Fe-X-C alloys

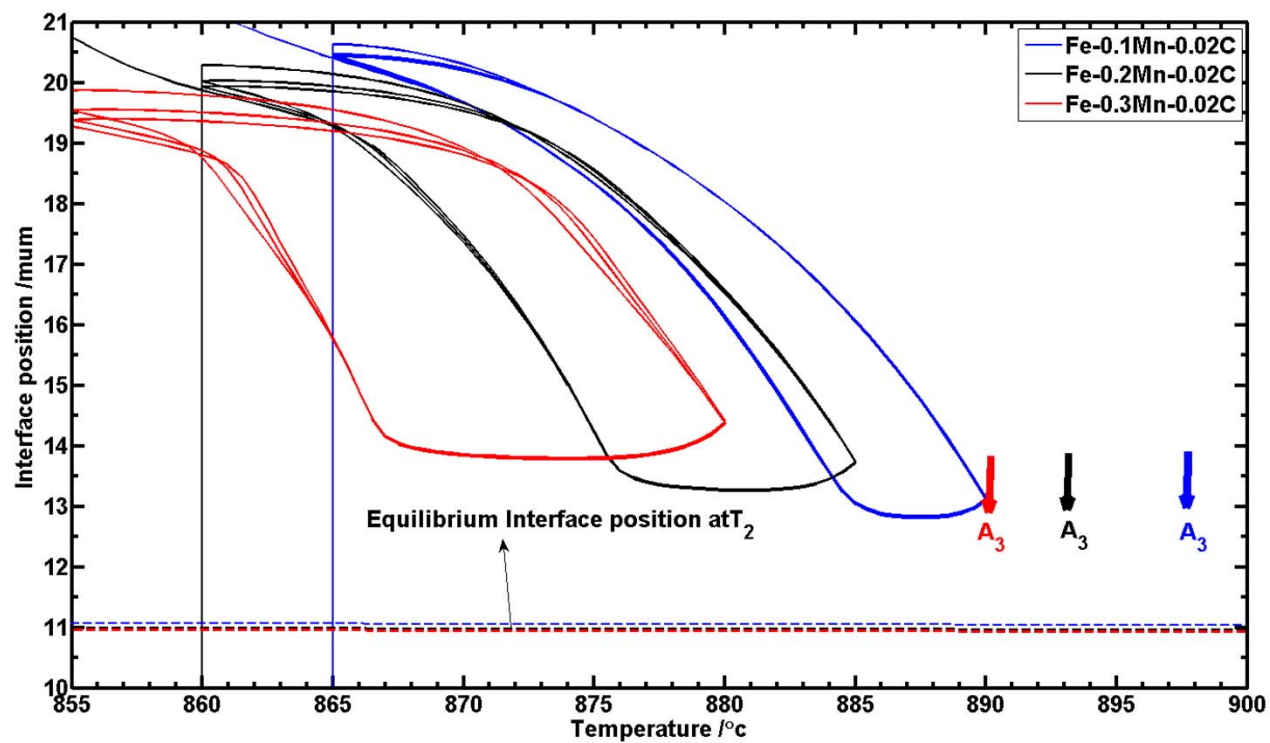
# Fe-Mn-C

Cycling temperatures fixed

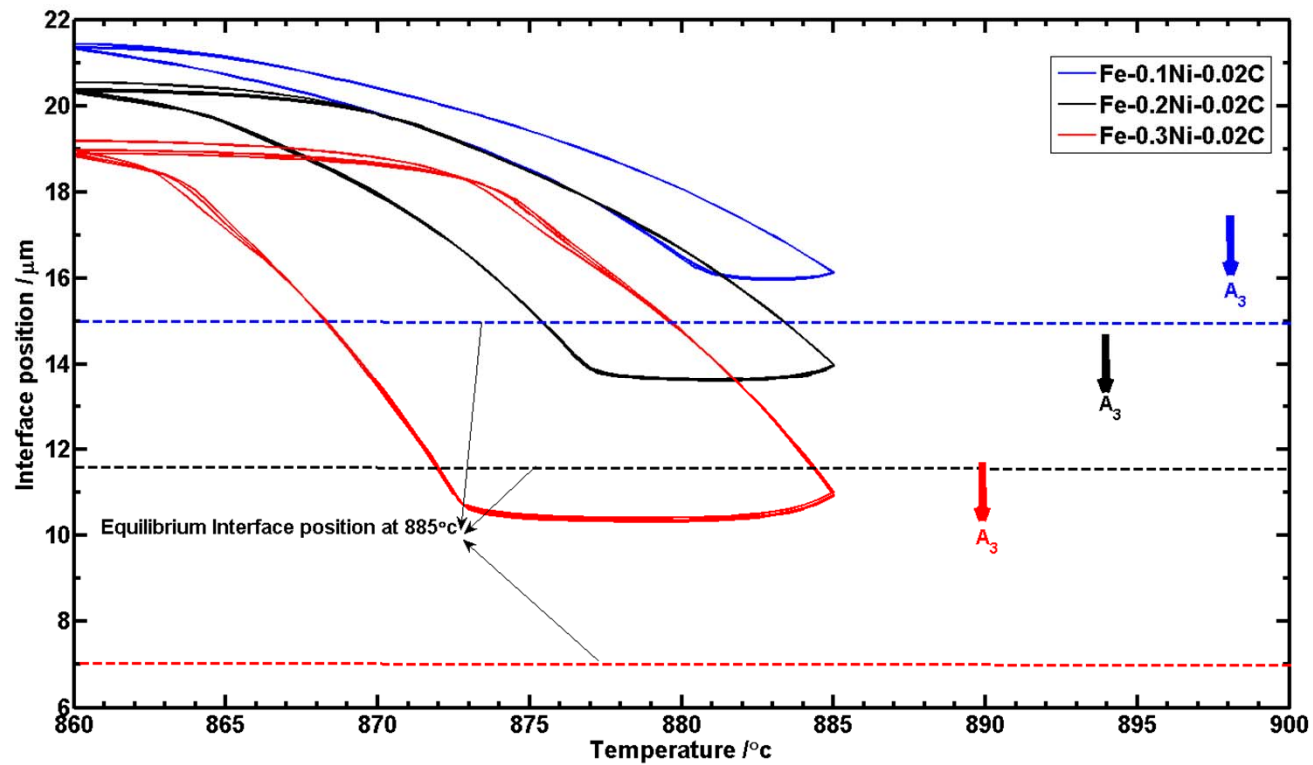


# Fe-Mn-C

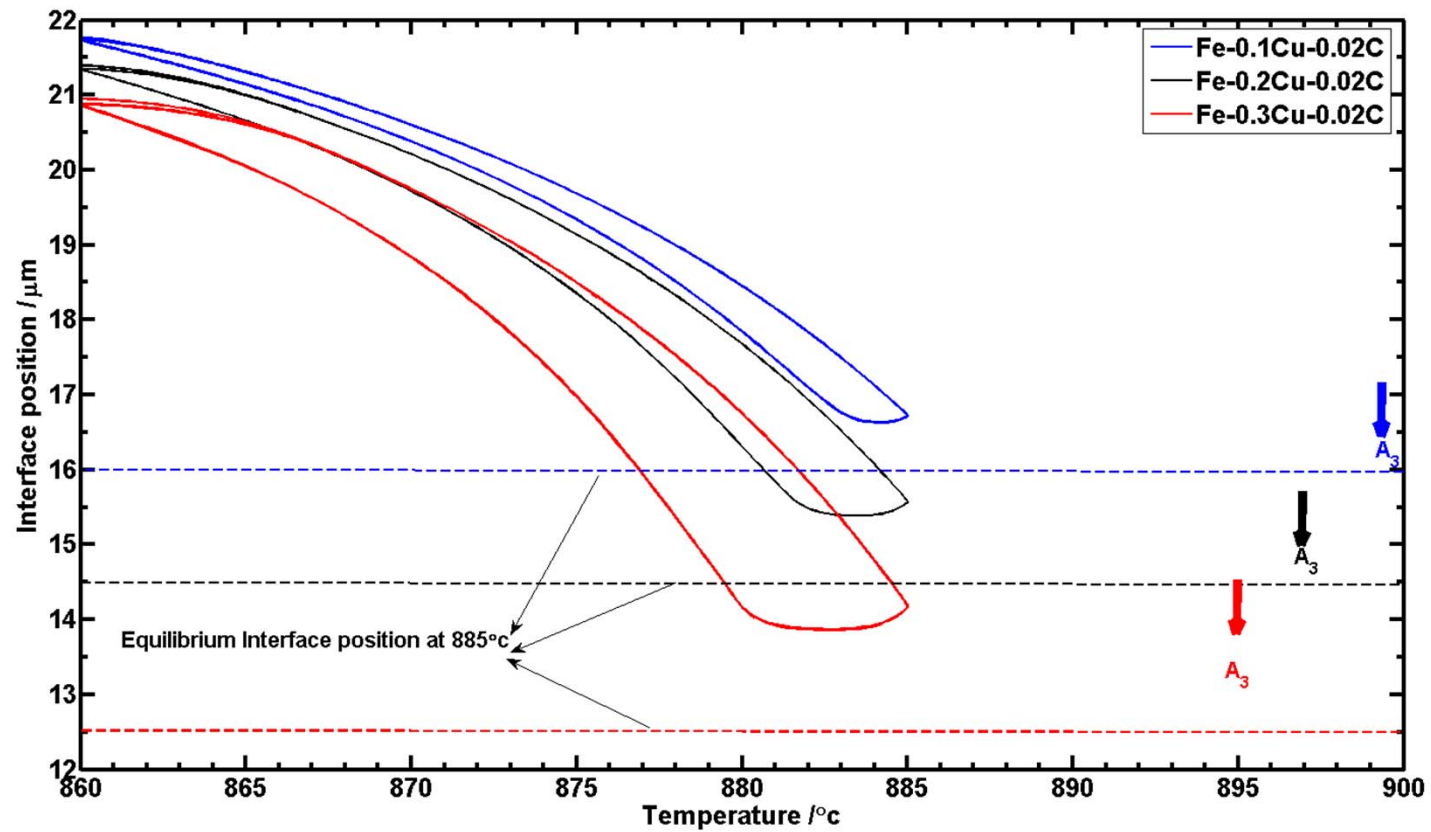
## Equilibrium fraction fixed



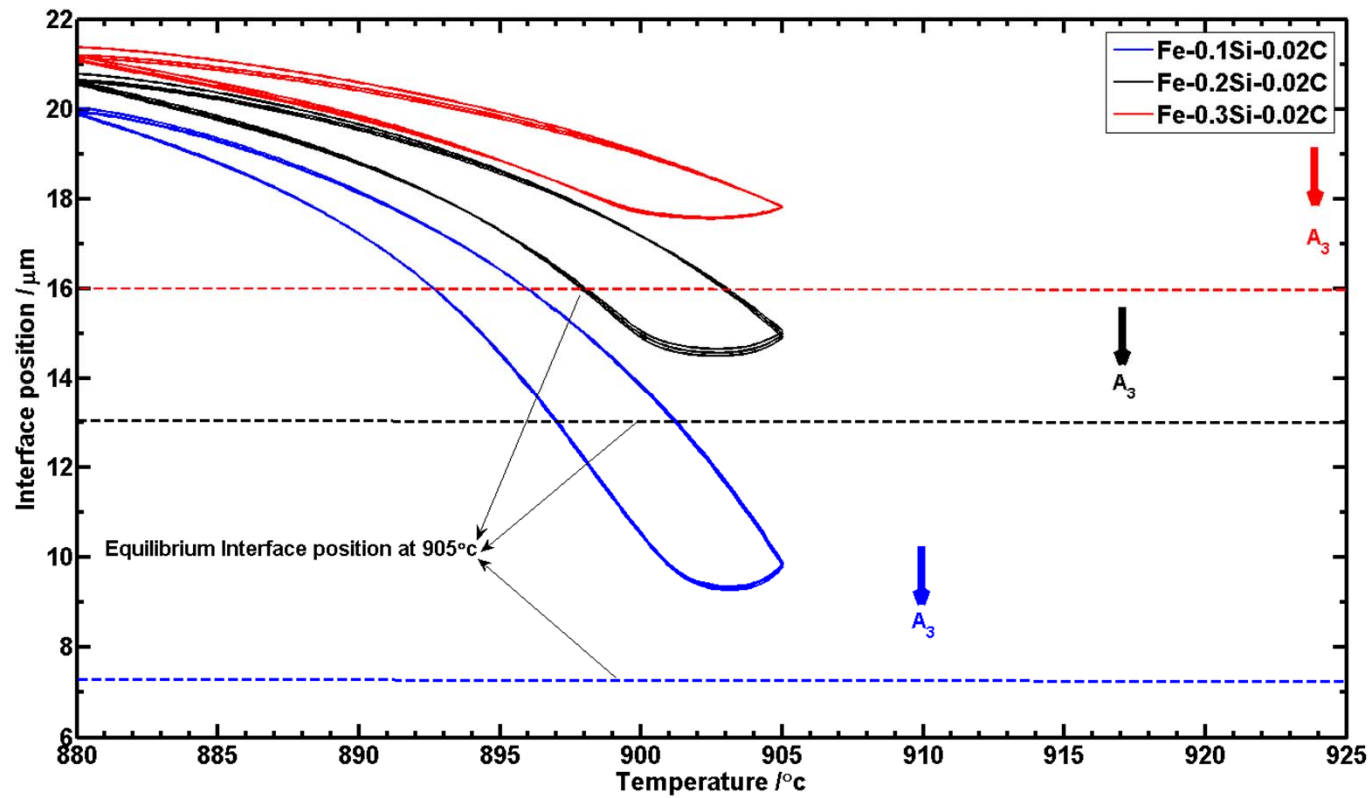
# Fe-Ni-C



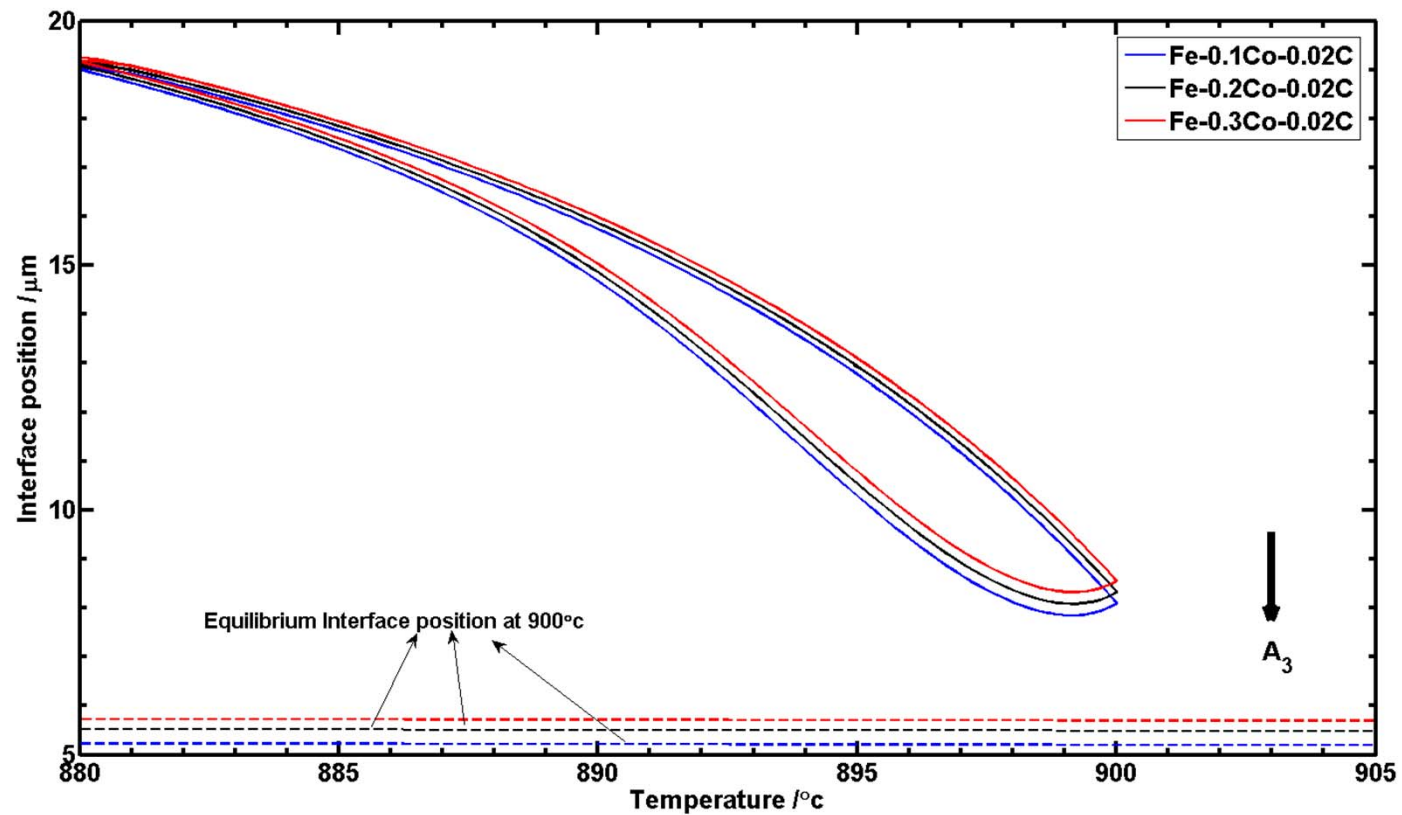
# Fe-Cu-C



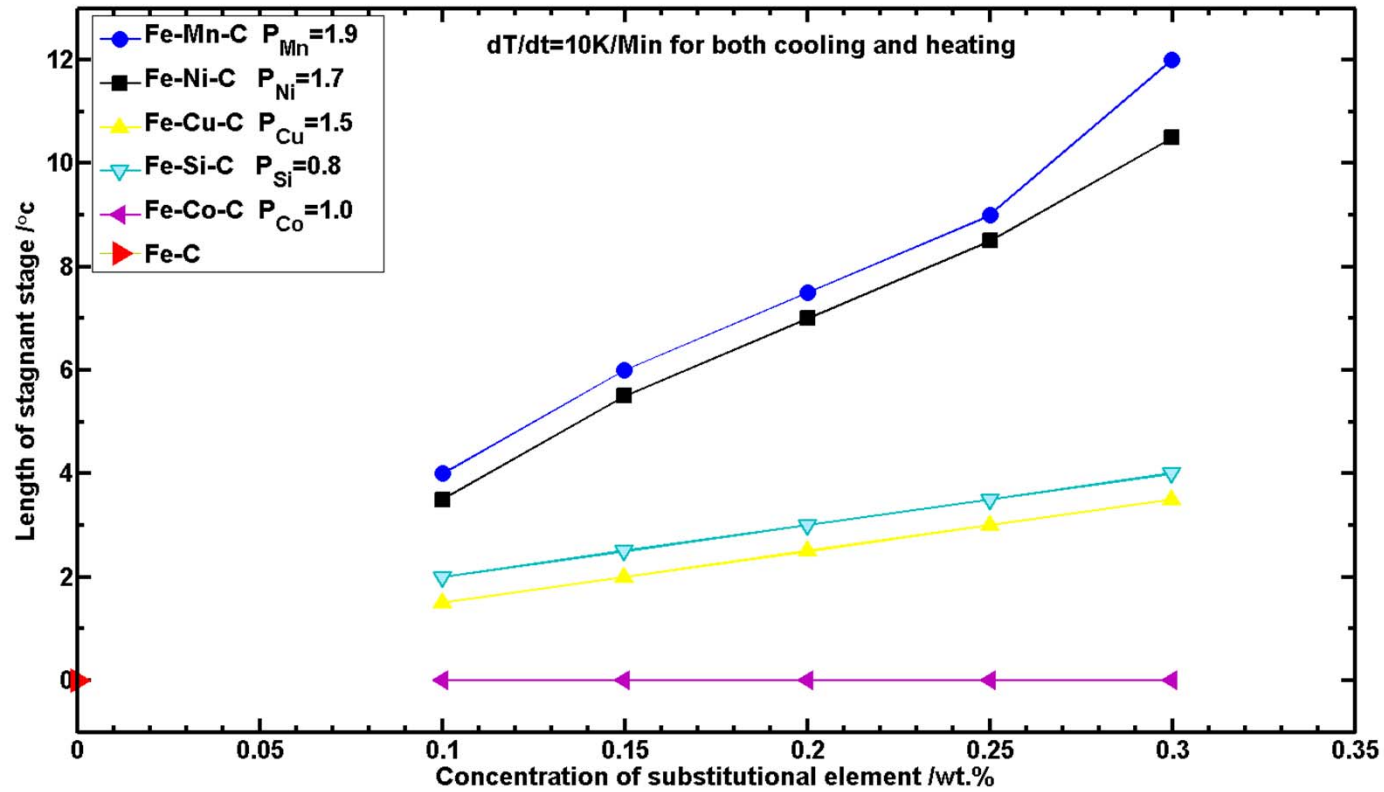
# Fe-Si-C



# Fe-Co-C



# Summarize

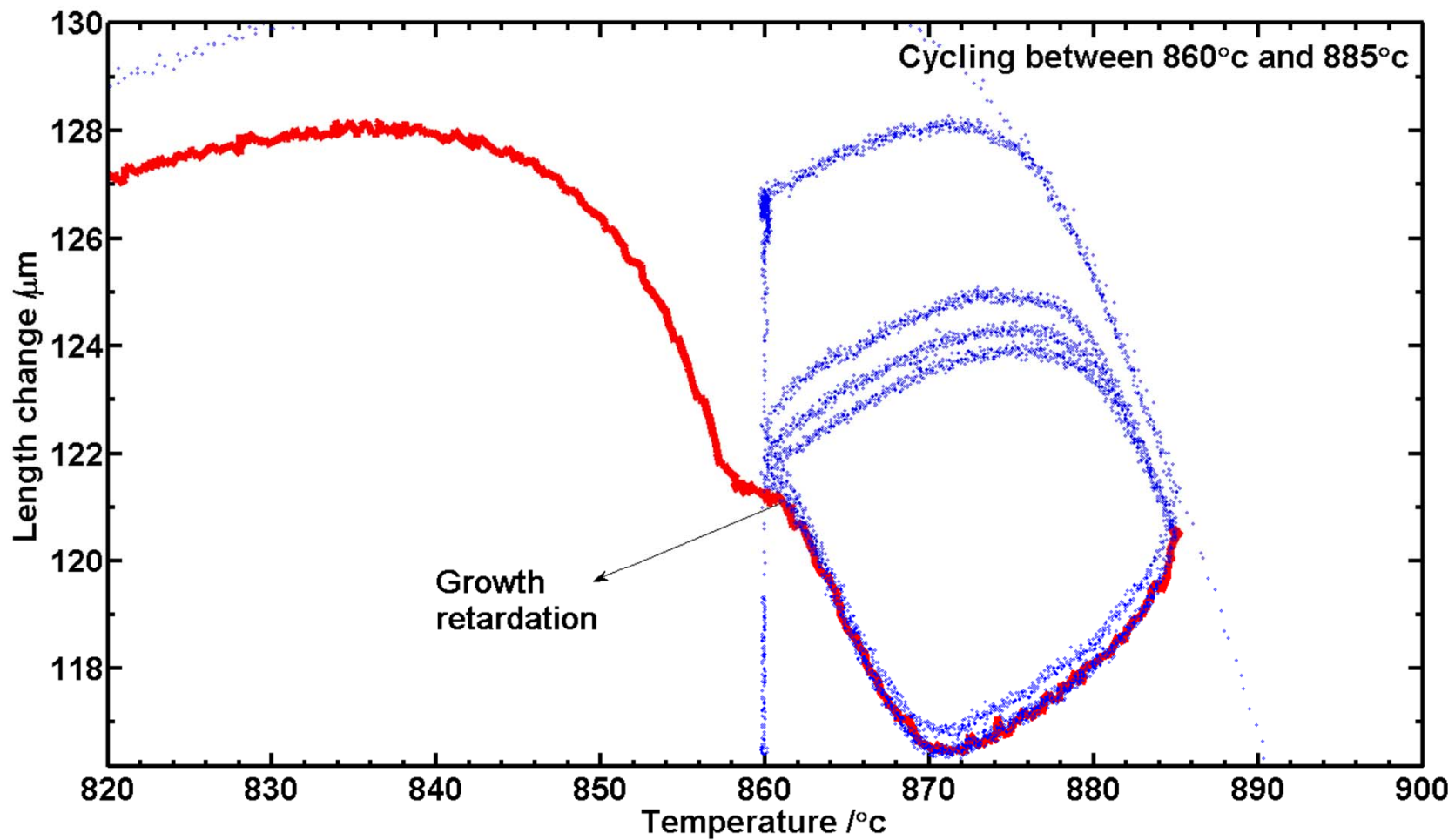


# Interim summary

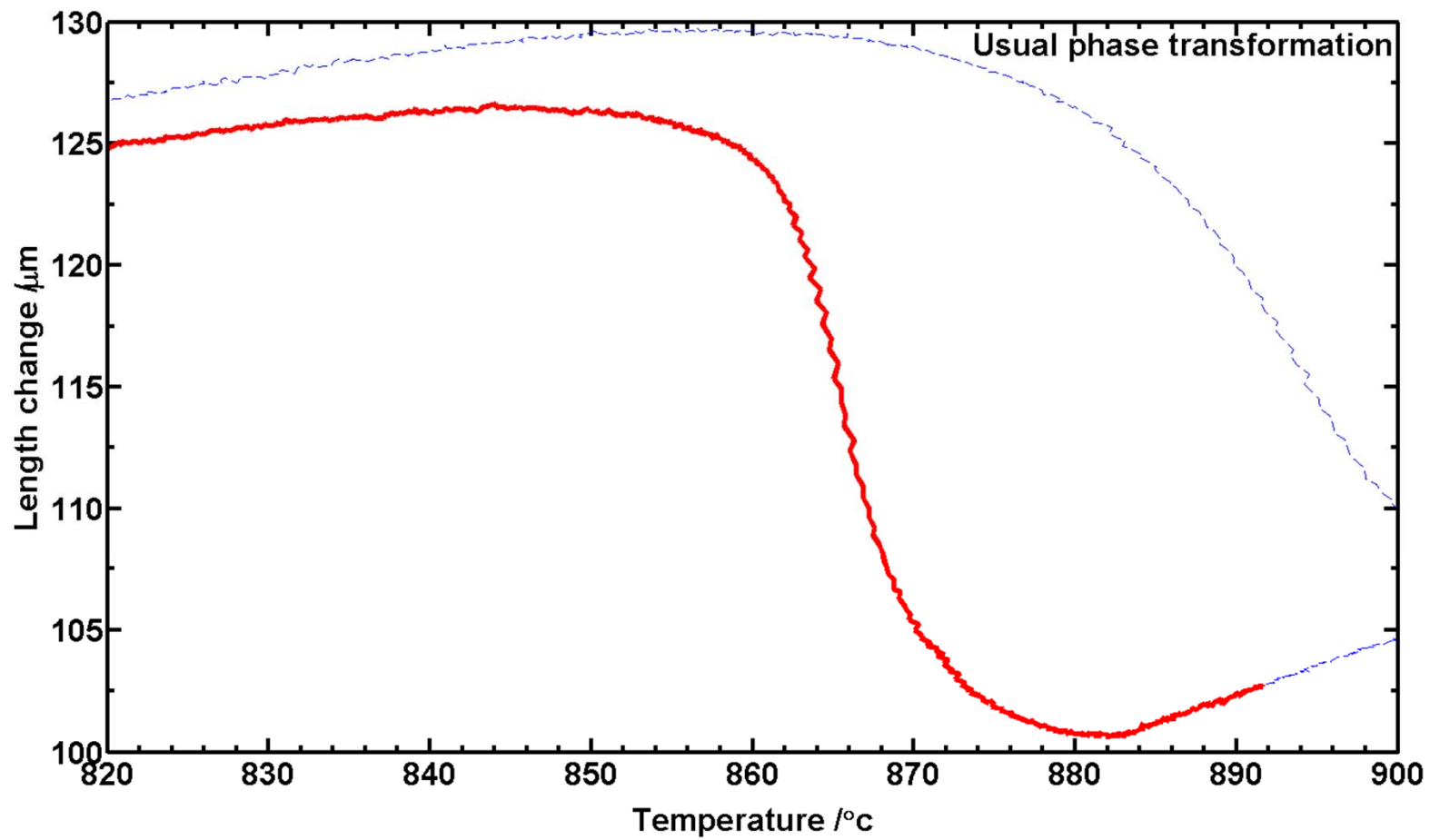
The length of stagnant stage is determined by the composition of substitutional elements and their partitioning coefficients.

# Creating evidence for the existence of the Mn –spike after cyclic transformations

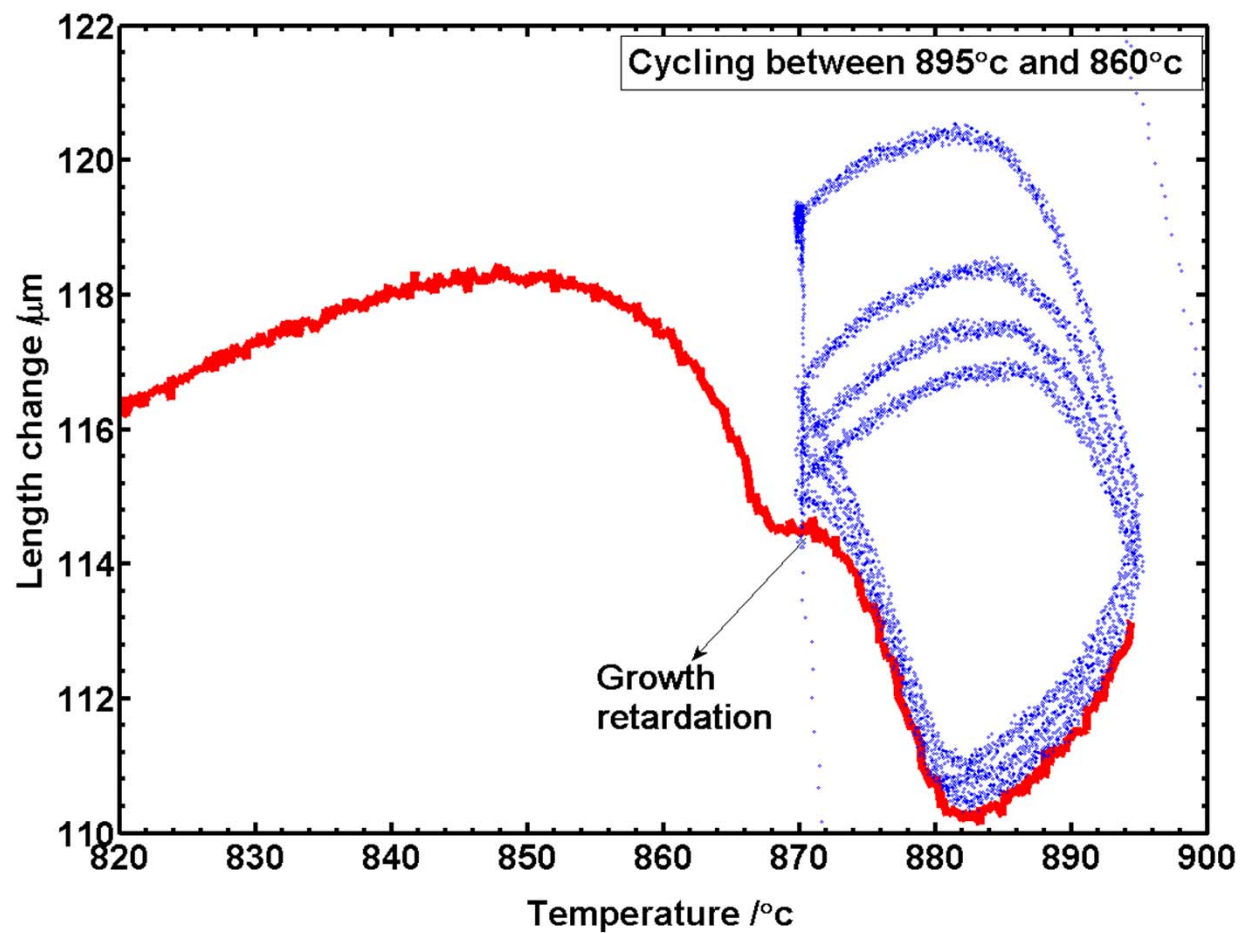
# Experiments



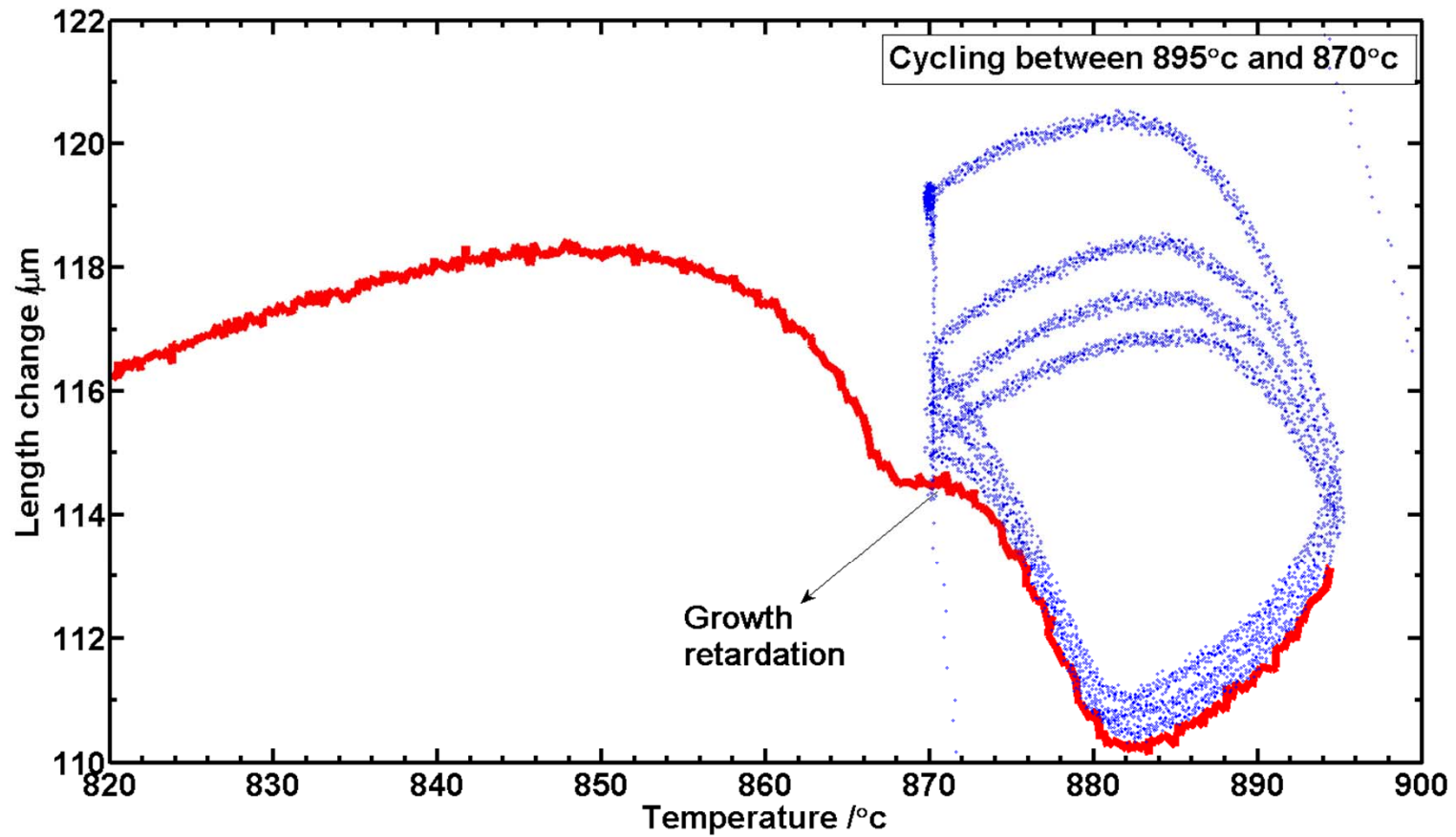
# Experiments



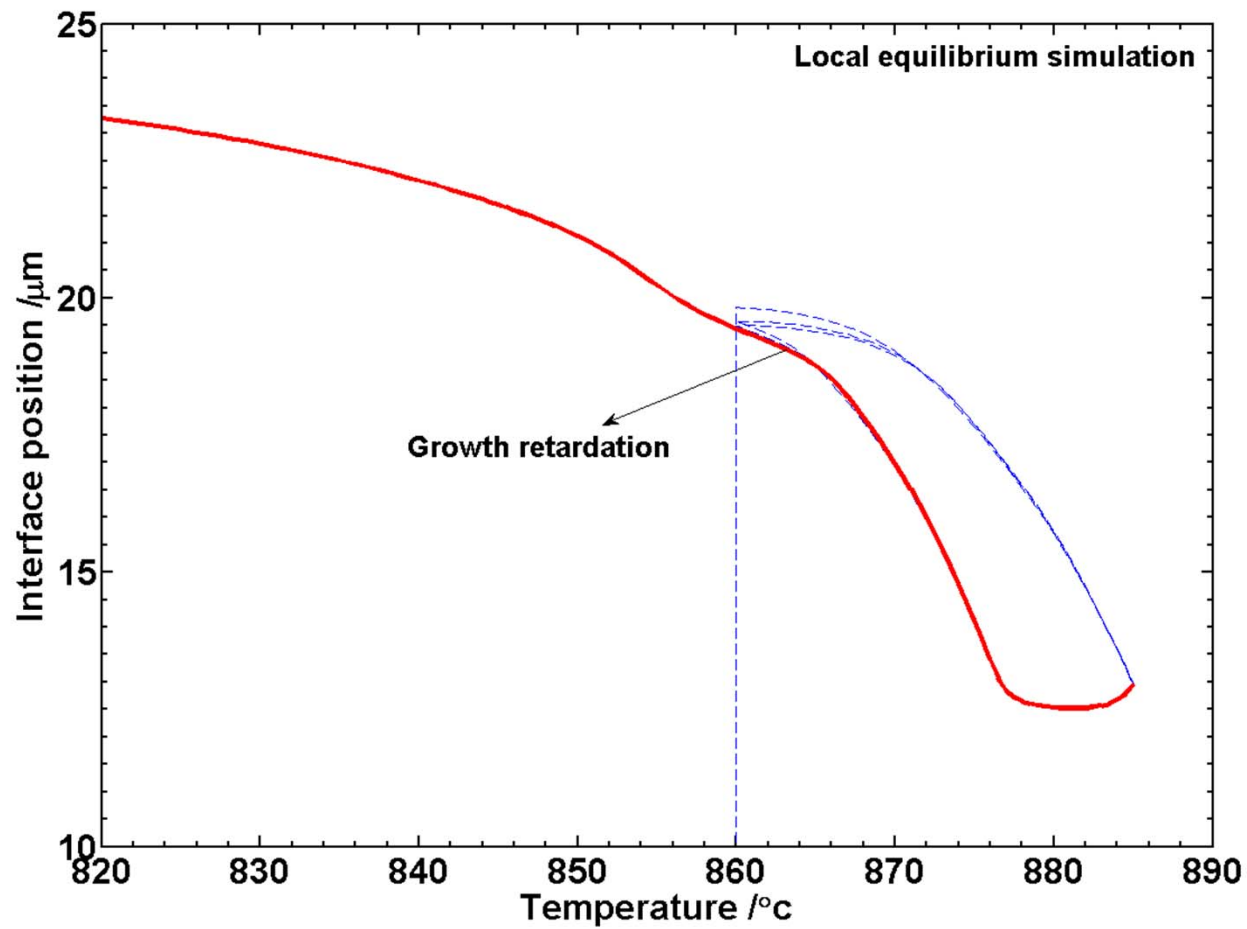
# Experiments



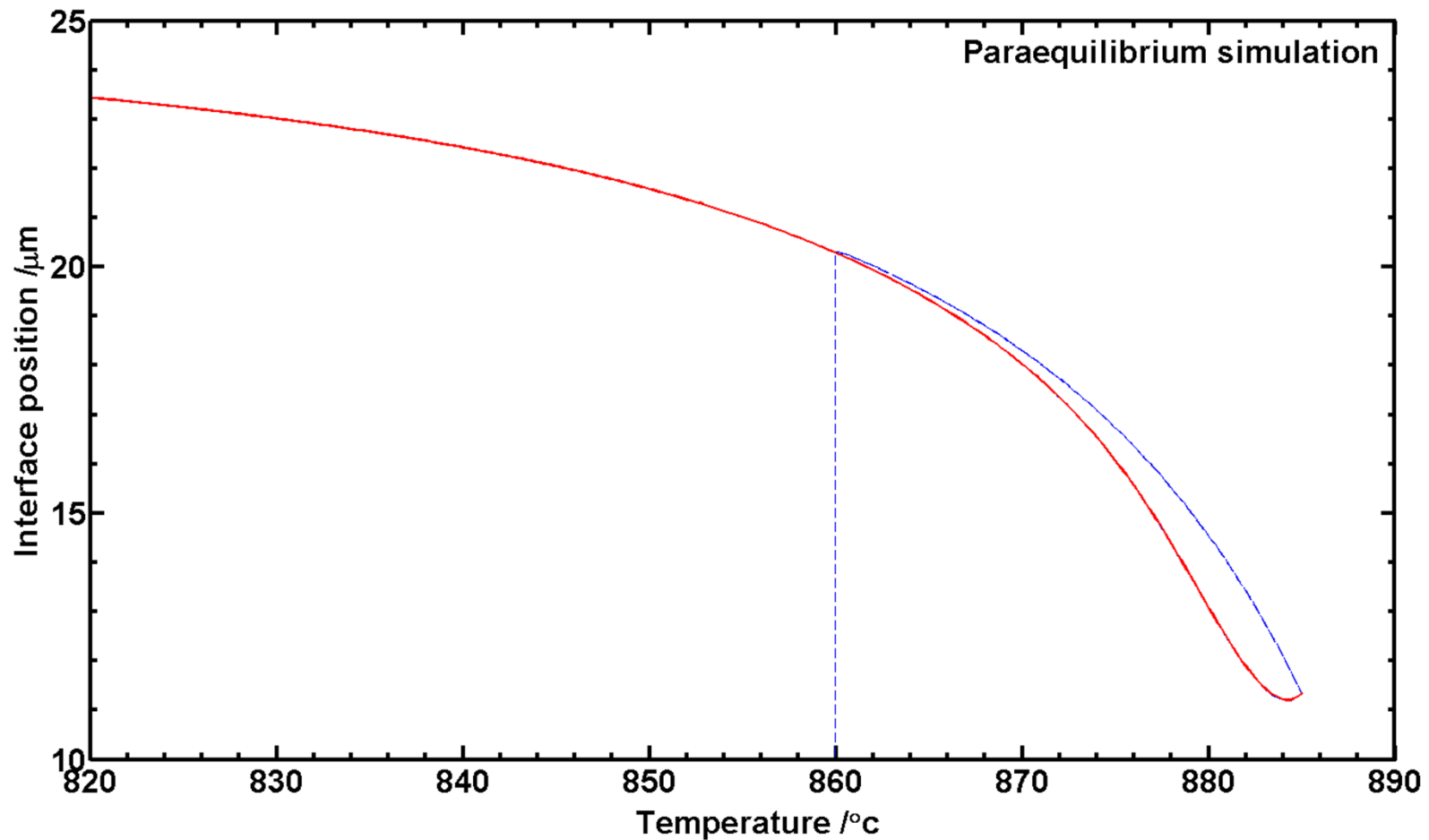
# Experiments



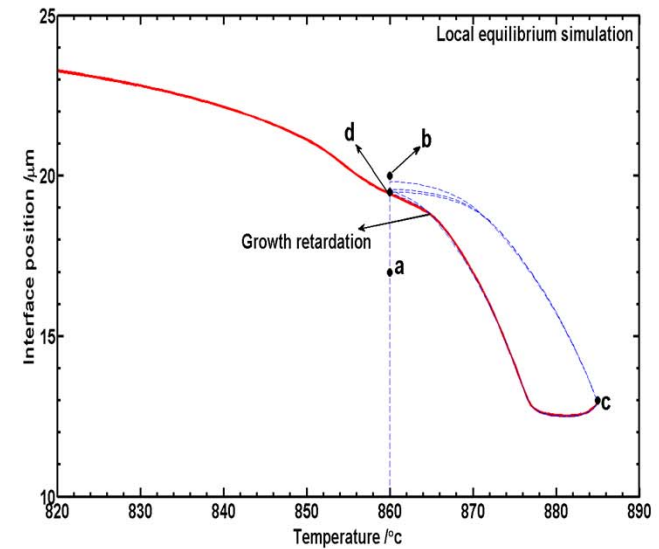
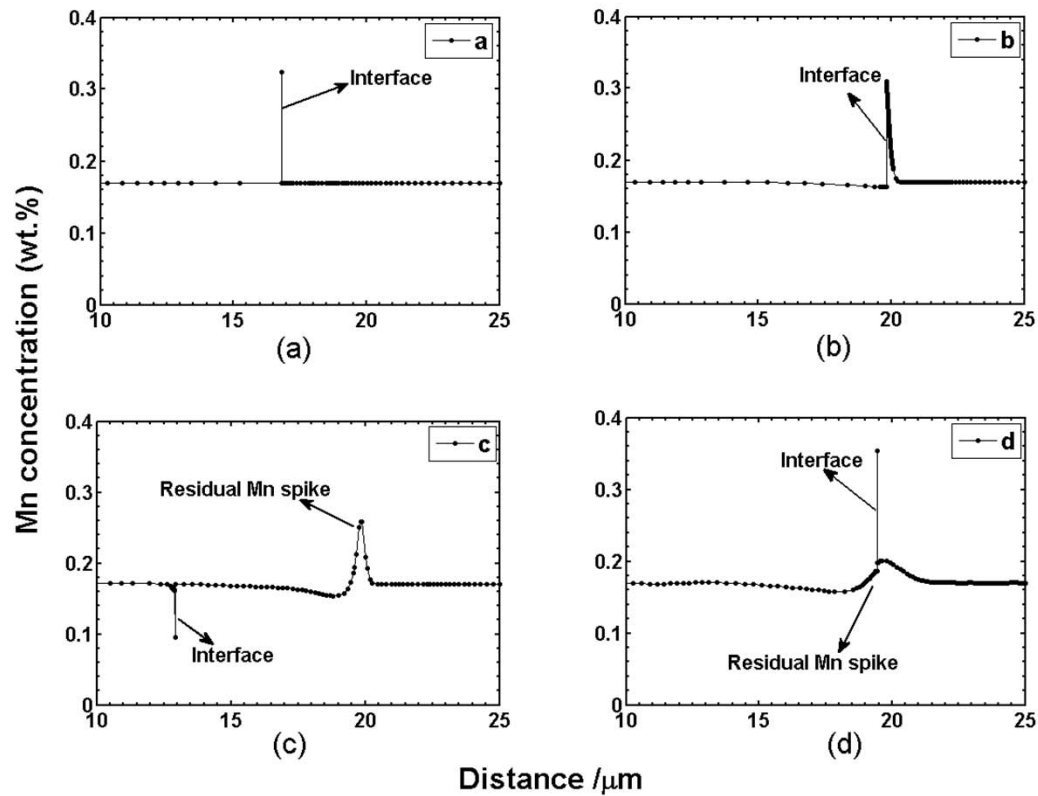
# Modeling



# Modeling



# Mn profiles



# Conclusion for the stagnant stage

1. The stagnant stage is attributed to growth kinetics issue rather than nucleation incubation.
2. LENP model considering Mn partitioning is more effective than the PE model.
3. The length of stagnant stage is determined by the interface conditions, partitioning coefficients of substitutional elements, and composition of substitutional elements.

# Conclusions as to the inverse transformation stage

1. The inverse phase transformation stage is caused by the non-equilibrium conditions at the transition temperatures
2. The duration of inverse phase transformation stage is determined by the interface conditions at the transition temperature, while the magnitude of inverse transformation is determined by both interface conditions and cooling rate.

# Conclusions as to the wiggle stage

1. The wiggle growth during the final cooling has been both observed in simulation and experiments.
2. According to the simulated Mn profiles, the deceleration during cooling is probably due to the existence of the Mn spikes in the austenite.
3. More simulation and experiments are required to prove this point.

## 4 Overall conclusions

1. Cyclic partial transformation experiments offer interesting insight into solid state transformations. LENP fits the data best
2. The real interfacial mobility has not been determined yet, but we understand better how to get there
3. We have some new tools to control dual phase material production